

## Electronic Supporting information

### The folding of a metallopeptide

Ilaria Gamba,<sup>¶</sup> Gustavo Rama,<sup>¶</sup> Elisabeth Ortega-Carrasco,<sup>#</sup> Roberto Berardozi,<sup>†</sup> Víctor M. Sánchez-Pedregal,<sup>§</sup> Lorenzo Di Bari,<sup>†</sup> Jean-Didier Maréchal,<sup>#,\*</sup> M. Eugenio Vázquez<sup>§,\*</sup> and Miguel Vázquez López<sup>¶,\*</sup>

<sup>¶</sup> *Departamento de Química Inorgánica and Centro Singular de Investigación en Química Biolóxica e Materiais Moleculares (CIQUS). Universidade de Santiago de Compostela. 15782 Santiago de Compostela, Spain. Ph.: (+34) 881 815 736. E-mail: [miguel.vazquez.lopez@usc.es](mailto:miguel.vazquez.lopez@usc.es).*

<sup>#</sup> *Departament de Química, Universitat Autònoma de Barcelona, 08193 Cerdanyola (Barcelona); E-mail: [jeandidier.marechal@uab.es](mailto:jeandidier.marechal@uab.es)*

<sup>†</sup> *Dipartimento di Chimica e Chimica Industriale, Università di Pisa. via Moruzzi 3, 56124 Pisa, Italy; E-mail: [lorenzo.dibari@unipi.it](mailto:lorenzo.dibari@unipi.it)*

<sup>§</sup> *Departamento de Química Orgánica and Centro Singular de Investigación en Química Biolóxica e Materiais Moleculares (CIQUS). Universidade de Santiago de Compostela. 15782 Santiago de Compostela, Spain. E-mail: [eugenio.vazquez@usc.es](mailto:eugenio.vazquez@usc.es).*

### General

All reagents were acquired from commercial sources: Dimethylformamide (DMF) and Trifluoroacetic acid (TFA) were purchased from *Scharlau*, CH<sub>2</sub>Cl<sub>2</sub> from *Panreac*, CH<sub>3</sub>CN from *Merck*, and the coupling agents HBTU (O-Benzotriazole-*N,N,N',N'*-tetramethyl-uronium-hexafluorophosphate) and HATU (2-(1*H*-7-azabenzotriazol-1-yl)-1,1,3,3-tetramethyluronium hexafluorophosphate methanaminium) from *GL Biochem* (Shanghai) Ltd. All other chemicals were purchased from *Sigma-Aldrich* or *Fluka*. All solvents were dry and synthesis grade, unless specifically noted. (NH<sub>4</sub>)Fe<sub>2</sub>(SO<sub>4</sub>)<sub>2</sub>·6H<sub>2</sub>O [ammonium iron(II) sulfate or Mohr's salt], Co(ClO<sub>4</sub>)<sub>2</sub>·6H<sub>2</sub>O and Ni(ClO<sub>4</sub>)<sub>2</sub>·6H<sub>2</sub>O salts from *Sigma-Aldrich* were used as metal ion sources.

Reactions were followed by analytical RP-HPLC with an Agilent 1100 series LC/MS using a *Luna C18* (250 x 4.60 mm) analytical column from *Phenomenex*. Standard conditions for analytical RP-HPLC consisted on a linear gradient from 15% to 95% of solvent B for 30 min at a flow rate of 1 mL/min (A: water with 0.1% TFA, B: acetonitrile with 0.1% TFA). Compounds were detected by UV absorption at 222, 254 and 310 nm.

High-Performance Liquid Chromatography (HPLC) was performed using an *Agilent 1100* series Liquid Chromatograph Mass Spectrometer system. Analytical HPLC was run using a *Luna C18* (250 x 4.60 mm) reverse phase analytical column; compounds were detected by UV absorption at 222, 254 and 310 nm. The purification of the peptides was performed on a *Luna C18* (250 x 10 mm) semi-preparative reverse phase column from *Phenomenex*. The standard gradient used for analytical and semi-preparative HPLC was 90:10 to 50:50 over 30 min (water/acetonitrile, 0.1% TFA). Electrospray Ionization Mass Spectrometry (ESI/MS)

was performed with an *Agilent 1100 Series LC/MSD VL* model in positive scan mode using direct injection of the purified peptide solution into the MS.

Peptides purification was performed by semi-preparative RP-HPLC with an *Agilent 1100 series Liquid Chromatograph* using a *Luna 5u C<sub>18</sub>(2) 100A* (5 μm, 10 × 250 mm) reverse-phase column from *Phenomenex*. Standard conditions for analytical and semi-preparative RP-HPLC consisted on an isocratic regime during the first 5 min, followed by a linear gradient from 10% to 50% of solvent B for 30 min (A: water 0.1% TFA, B: acetonitrile 0.1% TFA). Compounds were detected by UV absorption (222 nm) and by ESI<sup>+</sup>-MS. The fractions containing the products were freeze-dried, and their identity was confirmed by ESI<sup>+</sup>-MS and MALDI-TOF.

Electrospray Ionization Mass Spectrometry (ESI/MS) was performed with an *Agilent 1100 Series LC/MS* model in positive scan mode using direct injection of the purified peptide solution into the MS. Matrix-assisted laser desorption/ionization mass spectrometry (MALDI/MS) was performed with a *Bruker Autoflex MALDI/TOF* model in positive scan mode by direct irradiation of the matrix-absorbed peptide.

UV measurements were made in a *Jasco V-630* spectrophotometer, and coupled to a *Jasco ETC-717* temperature controller, using a standard *Hellma* semi-micro cuvette (140.002-QS). Measurements were made at 25 °C.

Circular dichroism measurements were made with a *Jasco J-715* coupled to a *Neslab RTE-111* thermostated water bath, using a *Hellma* 100-QS macro cuvette (1 mm light pass).

## SPPS methodology

All peptide synthesis reagents and Fmoc amino acid derivatives were purchased from *GL Biochem* (Shanghai) Ltd. *Novabiochem*. Fmoc-O1Pen-OH was purchased from *IRIS Biotech* (Cat. #: FAA1565).

C-terminal amide peptides were synthesized following standard peptide synthesis protocols (Fmoc/tBu strategy) on a 0.1 mmol scale using a 0.20 mmol/g loading Fmoc-PAL-PEG-PS resin from *Life technologies* with a PS-3 automatic peptide synthesizer from *Protein Technologies*. The amino acids were coupled in 5-fold excess using HBTU as activating agent, except for the synthetic Fmoc-O1PenBpy-OH amino acid, which was coupled using HATU as activating agent.

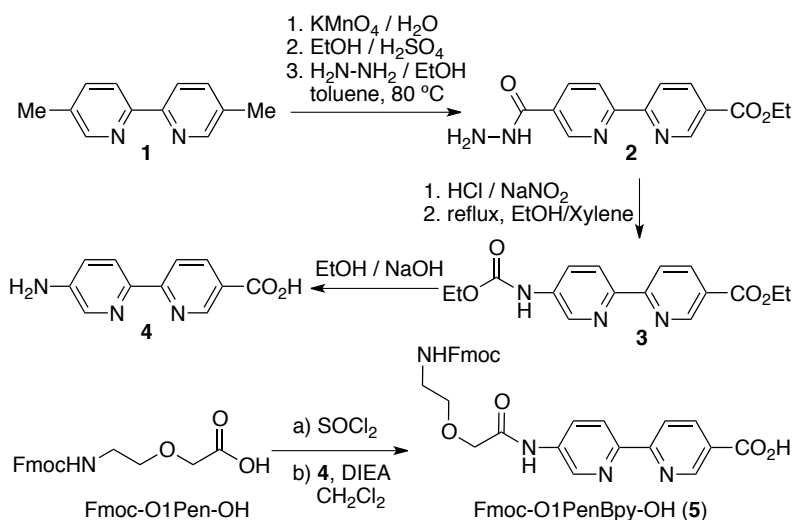
Each amino acid was activated for 30 seconds in DMF before being added onto the resin and couplings were conducted for 30 min. Deprotection of the temporal Fmoc protecting group was performed by treating the resin with 20% piperidine in DMF for 10 min.

**General procedure for cleavage-deprotection:** A resin-bound peptide dried overnight (0.025 mmol) was placed in a 50 mL falcon tube, to which 3 mL of the cleavage cocktail (50  $\mu$ L CH<sub>2</sub>Cl<sub>2</sub>, 25  $\mu$ L of H<sub>2</sub>O, 25  $\mu$ L of TIS (Triisopropylsilane) and 940 TFA  $\mu$ L) were added. The resulting suspension was shaken for 3 h. The resin was filtered, and the TFA filtrate was concentrated with an nitrogen current to an approximate volume of 1 mL, which was added to ice-cold diethyl ether (10 mL). After 10 min, the precipitate was centrifuged and washed again with 15 mL of ice-cold ether. The solid residue was dried under argon and redissolved in acetonitrile/water 1:1 (1 mL) and purified by semi-preparative reverse-phase HPLC. The collected fractions were lyophilized and stored at -20 °C. Their identity was confirmed by ESI<sup>+</sup>-MS and MALDI-TOF.

## Synthesis of Fmoc-O1PenBpy-OH

The bipyridine amino acid was obtained following the route previously reported by us,<sup>1</sup> and which is based on a method reported by Newkome *et al.*<sup>2</sup>, starting from 5,5'-diethyl-2,2'-bipyridine, which was obtained from 5,5-dimethyl-2,2'-bipyridine using the method reported by Francis H. Case<sup>3</sup> and Whittle *et al.*<sup>4</sup>

- 
- (1) Rama, G; Ardá, A.; Maréchal, J.-D.; Gamba, I.; Ishida, H.; Jiménez-Barbero, J.; Vázquez, M. E.; Vázquez López, M. *Chem. Eur. J.*, **2012**, *18*, 7030-7035.
  - (2) Newkome, G. R.; Gross, J.; Patri, A. K. *J. Org. Chem.* **1997**, *62*, 3013-3014.
  - (3) Francis H. Case, *J. Am. Chem. Soc.* **1946**, *68*, 2574-2577.
  - (4) Whittle C. P., *J. Heterocyclic Chem.* **1977**, *14*, 191-194.



**2,2'-bipyridine-5,5'-dicarboxylic acid.** A mixture of 39 g of potassium permanganate and 7 g of 5,5'-dimethyl-2,2'-bipyridine in 250 mL was heated for 2 h ( $115^\circ\text{C}$ ), cooled at rt and filtered through celite. The filtrate was cooled to  $4^\circ\text{C}$  and acidified with  $\text{HCl}(\text{aq})$  until precipitation of a white solid, which was filtered, washed with water and dried to give the desired product in 93% yield (8.7 g).  $^1\text{H-NMR}$  (500 MHz,  $\text{DMSO-d}_6$ ,  $\delta$ ): 13.50 (br); 9.18 (dd,  $^4J = 2.15$ ,  $^5J = 0.8$  Hz, 2H); 8.55 (dd,  $^3J = 8.3$ ;  $^5J = 0.8$  Hz, 2H); 8.44 (dd,  $^3J = 8.3$ ;  $^4J = 2.15$  Hz, 2H).  $^{13}\text{C-NMR}$  (125 MHz,  $\text{DMSO-d}_6$ ,  $\delta$ ): 165.49, 156.84, 149.82, 137.97, 126.65, 120.62. MALDI-TOF ( $m/z$ )  $[\text{M}+\text{H}]^+$  calcd. for  $[\text{C}_{12}\text{H}_8\text{N}_2\text{O}_4]$  245.0; found 245.0.

**5,5'-diethyl-2,2'-bipyridine.** [2,2'-bipyridine]-5,5'-dicarboxylic acid (10.0 g, 41 mmol) was suspended in 150 mL of absolute  $\text{EtOH}$ . Concentrated  $\text{H}_2\text{SO}_4$  acid (20.0 mL) was slowly added, and the resulting mixture was refluxed for 18 h. The solution was cooled to rt and added over 400 mL of water at  $4^\circ\text{C}$  until the precipitation of a white solid, which was filtered, washed with water and dried. 11.5 g (93.0%).  $^1\text{H-NMR}$  (500 MHz,  $\text{DMSO-d}_6$ ,  $\delta$ ): 9.20 (dd,  $^4J = 2.15$ ,  $^5J = 0.8$  Hz, 2H); 8.57 (dd,  $^3J = 8.3$ ;  $^5J = 0.8$  Hz, 2H); 8.46 (dd,  $^3J = 8.3$ ;  $^4J = 2.15$  Hz, 2H); 4.0 (q,  $^3J = 7.1$  Hz, 4H); 1.37 (t,  $^3J = 7.1$  Hz, 6H).  $^{13}\text{C-NMR}$  (125 MHz,  $\text{DMSO-d}_6$ ,  $\delta$ ): 164.2, 157.2, 149.8, 138.0, 126.2, 121.0, 61.1, 13.9. MALDI-TOF ( $m/z$ )  $[\text{M}+\text{H}]^+$  calcd. for  $[\text{C}_{16}\text{H}_{16}\text{N}_2\text{O}_4]$  301.1; found 301.1

**Ethyl 5'-Carbohydrazido-2,2'-bipyridine-5-carboxylate (2).** A mixture of diethyl 2,2'-bipyridine-5,5'-dicarboxylate (15.00 g, 50 mmol) and hydrazine hydrate (3.75 mL, 55 mmol) in a solution of  $\text{EtOH}$  (42 mL) and toluene (128 mL) was heated at  $80^\circ\text{C}$  for 48 h. The precipitate was filtered, washed with  $\text{CHCl}_3$  and dried in vacuum 11.4 g (80%). The unreacted diethyl ester was concentrated and reacted again to obtain a global yield of (90%).  $^1\text{H-NMR}$  (500 MHz,  $\text{DMSO-d}_6$ ,  $\delta$ ): 1.35 (t, 3H), 4.37 (q, 2H), 8.35 (d,  $^3J = 8.4$  Hz, 1H), 8.45 (dd,  $^3J = 8.4$  Hz,  $^4J = 2$  Hz, 1H), 8.52 (d,  $^3J = 8.4$  Hz, 1H), 8.57 (d,  $^3J = 8.4$  Hz, 1H), 9.1 (d,  $^4J = 2$  Hz, 1H), 9.2 (d,  $^4J = 2$  Hz, 1H), 10.1 (br, 1H).  $^{13}\text{C-NMR}$  (125 MHz,  $\text{DMSO-d}_6$ ,  $\delta$ ): 14.1, 61.3, 120.9, 120.9, 126.1, 129.6, 136.2, 138.2, 148.1, 150.0, 155.8, 157.8, 163.8, 164.5. MALDI-TOF ( $m/z$ )  $[\text{M}+\text{H}]^+$  calcd. for  $[\text{C}_{14}\text{H}_{14}\text{N}_4\text{O}_3]$  287.1; found 287.1.

**Ethyl 5'-Carbazido-2,2'-bipyridine-5-carboxylate.** A solution of 5-(ethoxycarbonyl)-5'-carbohydrazido-2,2'-bipyridine (5.7 g, 20 mmol) in concentrated  $\text{HCl}$  (100 mL) was cooled to  $0^\circ\text{C}$ . Aqueous  $\text{NaNO}_2$  (1.73 g, 25 mmol; 15 mL) was added dropwise maintaining the temperature  $0^\circ\text{C}$ . After 60 min, the resulting yellow solution was diluted with water (300 mL) to precipitate the monoester 5 as a colorless powder, which was

filtered, washed with water, and dried. 5.5 g (92 %). <sup>1</sup>H-NMR (500 MHz, Acetone-d<sub>6</sub>, δ): 9.13 (d, <sup>4</sup>J = 1.91 Hz, 1H), 9.10 (d, <sup>4</sup>J = 1.91 Hz, 1H), 8.71 (d, <sup>3</sup>J = 12.5 Hz, 1H), 8.69 (d, <sup>3</sup>J = 12.5 Hz, 1H), 8.517 (m, 2H); 4.31 (q, <sup>3</sup>J = 7.15 Hz, 2H); 1.29 (t, <sup>3</sup>J = 7.15, 3H). <sup>13</sup>C-NMR (125 MHz, Acetone-d<sub>6</sub>, δ): 170.8, 164.5, 159.2, 157.7, 150.3, 150.0, 138.0, 137.9, 127.0, 121.3, 61.2, 13.6. MALDI-TOF (*m/z*) [M+H]<sup>+</sup> calcd. for [C<sub>14</sub>H<sub>11</sub>N<sub>5</sub>O<sub>3</sub>] 298.1; found 298.1

**Ethyl-5'-(Ethoxycarbonyl)amino-2,2'-bipyridine-5-carboxylate (3)** A solution of ethyl 5'-carbazido-2,2'-bipyridine-5-carboxylate (8.6 g, 29 mmol) in a mixture of EtOH (100 mL) and xylene (100 mL) was heated at 90 °C for 4 h. The solvent was evaporated under reduced pressure, and the yellow residue was washed with EtOH and dried *in vacuo*. 8.21 g (90%). <sup>1</sup>H-NMR (500 MHz, DMSO-d<sub>6</sub>, δ): 1.27 (t, *J* = 7.2 Hz, 3H), 1.35 (t, *J* = 7.2 Hz, 3H), 4.17 (q, *J* = 7.2 Hz, 2H), 4.36 (q, *J* = 7.2 Hz, 2H), 8.08 (dd, <sup>3</sup>J = 8 Hz, <sup>4</sup>J = 2 Hz, 1H), 8.35 (dd, <sup>3</sup>J = 8.3 Hz, <sup>4</sup>J = 2 Hz, 1H), 8.40 (dd, <sup>3</sup>J = 8.3 Hz, <sup>5</sup>J = 1 Hz, 1H), 8.45 (d, <sup>3</sup>J = 8 Hz, 1H), 8.70 (d, <sup>4</sup>J = 2 Hz, 1H), 9.12 (d, <sup>4</sup>J = 2 Hz, <sup>5</sup>J = 1 Hz, 1H), 10.13 (s, 1H). <sup>13</sup>C-NMR (125 MHz, DMSO-d<sub>6</sub>, δ): 13.6, 13.9, 60.3, 60.6, 119.1, 121.2, 124.46, 124.9, 136.7, 137.4, 139.0, 147.4, 149.4, 153.1, 158.1, 164.2. MALDI-TOF (*m/z*) [M+H]<sup>+</sup> calcd. for [C<sub>16</sub>H<sub>17</sub>N<sub>3</sub>O<sub>4</sub>] 316.1; found 316.1

**5'-Amino-2,2'-bipyridine-5-carboxylic Acid Hydrochloride (4)** A solution of ethyl 5'-[(ethoxycarbonyl)amino]-2,2'-bipyridine-5-carboxylate (14.55 g, 45.9 mmol) in EtOH (50 mL) and 2.5 N aqueous NaOH (50 mL) was heated at 75 °C for 14 h. The EtOH was concentrated under reduced pressure and the resulting aqueous solution was acidified with HCl to afford a bright yellow precipitate, which was filtered, washed with cold water, and dried. 9.80 g (85%). <sup>1</sup>H-NMR (500 MHz, D<sub>2</sub>O, δ): 7.00 (dd, <sup>3</sup>J = 8.5 Hz, <sup>4</sup>J = 2.8 Hz, 1H), 7.55, 7.61 (d, <sup>3</sup>J = 8.5 Hz, 2H), 7.81 (d, <sup>4</sup>J = 2.9 Hz, 1H), 7.98 (dd, <sup>3</sup>J = 8.5 Hz, <sup>4</sup>J = 2.9 Hz, 1H), 8.65 (d, <sup>4</sup>J = 2.8 Hz, 1H). <sup>13</sup>C-NMR (125 MHz, D<sub>2</sub>O, δ): 123.3d, 126.2, 126.7, 133.8, 139.8, 141.34, 147.5, 147.4, 152.4, 159.6, 176.04. MALDI-TOF (*m/z*) [M+H]<sup>+</sup> calcd. for [C<sub>11</sub>H<sub>9</sub>N<sub>3</sub>O<sub>2</sub>] 216.1; found 216.1

**5'-(2-(2-(((9H-fluoren-9-yl)methoxy)carbonyl)amino)ethoxy)acetamido)-[2,2'-bipyridine]-5-carboxylic acid (Fmoc-O1PenBpy-OH, 5)** Fmoc-O1Pen-OH 10 (5.02 g, 14.72 mmol) was dissolved in 10 mL of SOCl<sub>2</sub> at rt and the resulting solution was stirred for 30 min. The thionyl chloride was evaporated under reduced pressure and the yellow solid was washed with CH<sub>2</sub>Cl<sub>2</sub> and then dried. Compound 4 (3.7 g, 14.8 mmol), 20 mL of CH<sub>2</sub>Cl<sub>2</sub> and 5 mL of DIEA were added and the suspension was stirred at rt overnight. The solvent was evaporated, the residue was suspended in acetonitrile 0.1 %TFA/H<sub>2</sub>O (2:1), centrifuged and washed with acetonitrile and H<sub>2</sub>O and dried to give 6.70 g (84 %). <sup>1</sup>H-NMR (DMSO-*d*<sup>6</sup>) δ: 9.19 (s, 1H); 8.90 (s, 1H); 8.49 (1H); 8.49 (1H); 8.35 (2H); 8.24 (1H); 7.67 (1H); 7.60 (2H); 7.26 (4H); 4.36 (2H); 4.17 (1H); 4.14 (2H); 3.65 (2H); 3.40 (2H). <sup>13</sup>C-NMR (DMSO-*d*<sup>6</sup>) δ: 169.76, 168.62, 157.23, 150.94, 149.21, 144.74, 143.47, 142.27, 141.59, 140.28, 138.29, 138.08, 129.73, 128.09, 125.96, 122.14, 120.87, 120.79, 118.73, 110.34, 67.38, 63.77, 47.62, 41.71. MALDI-TOF (*m/z*) [M+H]<sup>+</sup> calcd. for [C<sub>30</sub>H<sub>26</sub>N<sub>4</sub>O<sub>6</sub>] 539.2; found 539.1

## Synthesis of the Peptide Ligands

All the peptide ligands were synthesized following the SPPS protocol described above.

**GL-P:** H-O1PenBpy-Gly-Gly-Gly-O1PenBpy-Gly-(L-Pro)-Gly-O1PenBpy-NH<sub>2</sub>

**GD-P:** H-O1PenBpy-Gly-Gly-Gly-O1PenBpy-Gly-(D-Pro)-Gly-O1PenBpy-NH<sub>2</sub>

13 mg, 42 % yield for 0.024 mmol scale

ESI-MS (*m/z*) [M+H]<sup>+</sup> calcd. for C<sub>60</sub>H<sub>67</sub>N<sub>19</sub>O<sub>15</sub> = 1294.3, found = 1294.2; [M+2H]<sup>2+</sup> 647.3

MALDI-TOF (*m*) [M+H]<sup>+</sup> calcd. for C<sub>60</sub>H<sub>67</sub>N<sub>19</sub>O<sub>15</sub> = 1294.3, found = 1294.5

UV (H<sub>2</sub>O) λ<sub>max</sub>, nm (ε): 308 (84850) M<sup>-1</sup>cm<sup>-1</sup>

**DL-P:** H-O1PenBpy-Gly-(D-Pro)-Gly-O1PenBpy-Gly-(L-Pro)-Gly-O1PenBpy-NH<sub>2</sub>

**LD-P:** H-O1PenBpy-Gly-(L-Pro)-Gly-O1PenBpy-Gly-(D-Pro)-Gly-O1PenBpy-NH<sub>2</sub>

11 mg, 34 % yield for 0.024 mmol scale

ESI-MS (*m/z*) [M+H]<sup>+</sup> calcd. for C<sub>63</sub>H<sub>71</sub>N<sub>19</sub>O<sub>15</sub> = 1334.4, found = 1334.5; [M+2H]<sup>2+</sup> 667.7

MALDI-TOF (*m*) [M+H]<sup>+</sup> calcd. for C<sub>63</sub>H<sub>71</sub>N<sub>19</sub>O<sub>15</sub> = 1334.4, found = 1334.5

UV (H<sub>2</sub>O) λ<sub>max</sub>, nm (ε): 308 (84850) M<sup>-1</sup>cm<sup>-1</sup>

**LL-P:** H-O1PenBpy-Gly-(L-Pro)-Gly-O1PenBpy-Gly-(L-Pro)-Gly-O1PenBpy-NH<sub>2</sub>

**DD-P:** H-O1PenBpy-Gly-(D-Pro)-Gly-O1PenBpy-Gly-(D-Pro)-Gly-O1PenBpy-NH<sub>2</sub>

16 mg, 50 % yield for 0.024 mmol scale

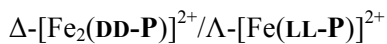
ESI-MS (*m/z*) [M+H]<sup>+</sup> calcd. for C<sub>63</sub>H<sub>71</sub>N<sub>19</sub>O<sub>15</sub> = 1334.4, found = 1334.5; [M+2H]<sup>2+</sup> 667.7

MALDI-TOF (*m*) [M+H]<sup>+</sup> calcd. for C<sub>63</sub>H<sub>71</sub>N<sub>19</sub>O<sub>15</sub> = 1334.4, found = 1334.5

UV (H<sub>2</sub>O) λ<sub>max</sub>, nm (ε): 308 (84850) M<sup>-1</sup>cm<sup>-1</sup>

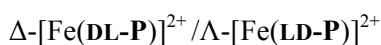
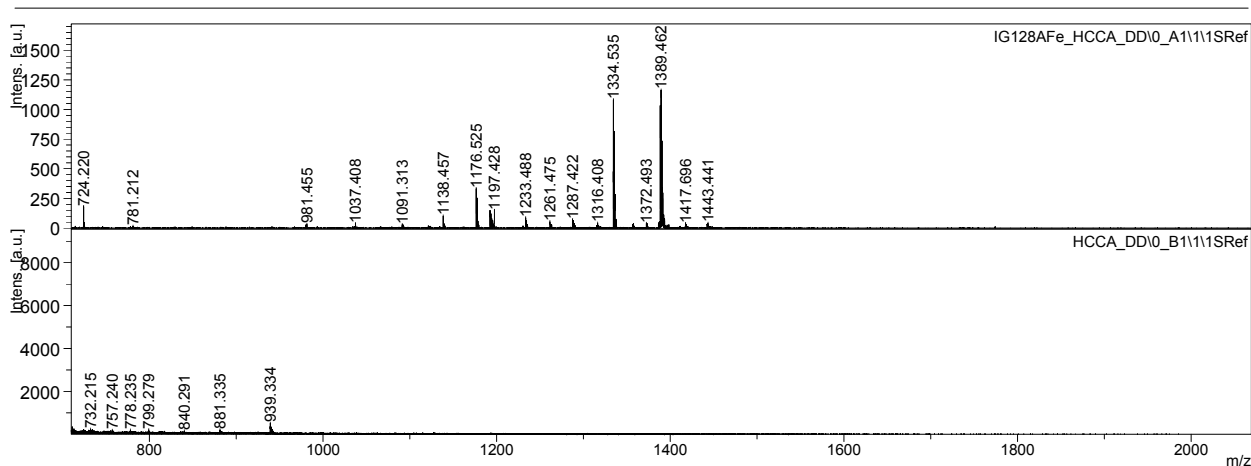
## Synthesis of the Fe(II) Metallopeptides

All the metallopeptides were synthesized by additions of aliquots of an 10mM aqueous solutions of  $(\text{NH}_4)_2\text{Fe}(\text{SO}_4)_2 \cdot 6\text{H}_2\text{O}$  to an aqueous solution of the corresponding free peptide ligand in PBS buffer (10 mM) at pH 5.6 (293 K). The formation of the ML species was followed by UV/Vis titration experiments.



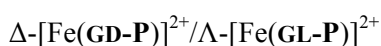
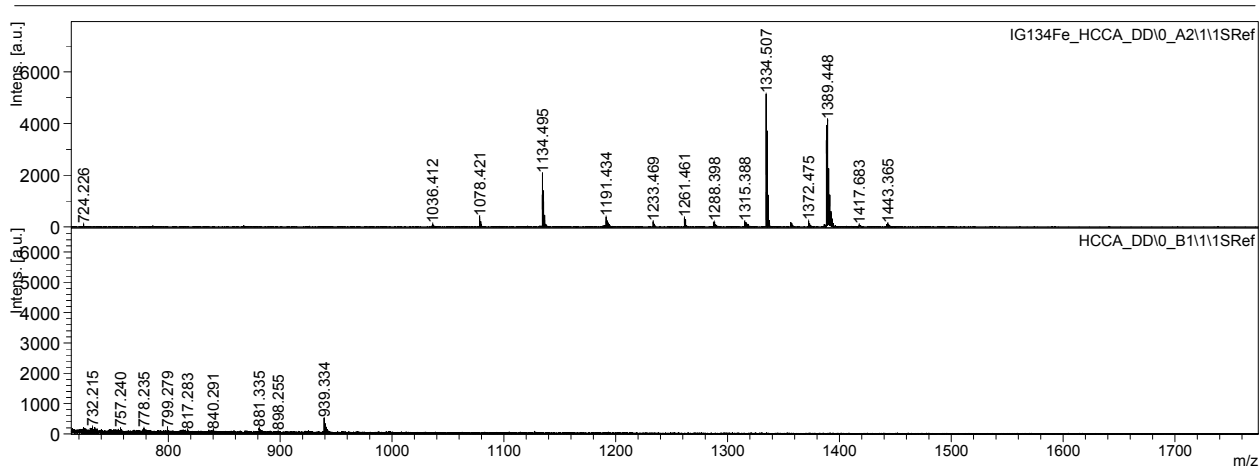
MALDI-TOF ( $m/z$ )  $[\text{M}]^+$  calc for  $\text{C}_{63}\text{FeH}_{71}\text{N}_{19}\text{O}_{15} = 1390.2$ , found = 1389.4

UV ( $\text{H}_2\text{O}$ )  $\lambda_{\text{max}}$ , nm ( $\epsilon$ ): 540 (5325)  $\text{M}^{-1}\text{cm}^{-1}$



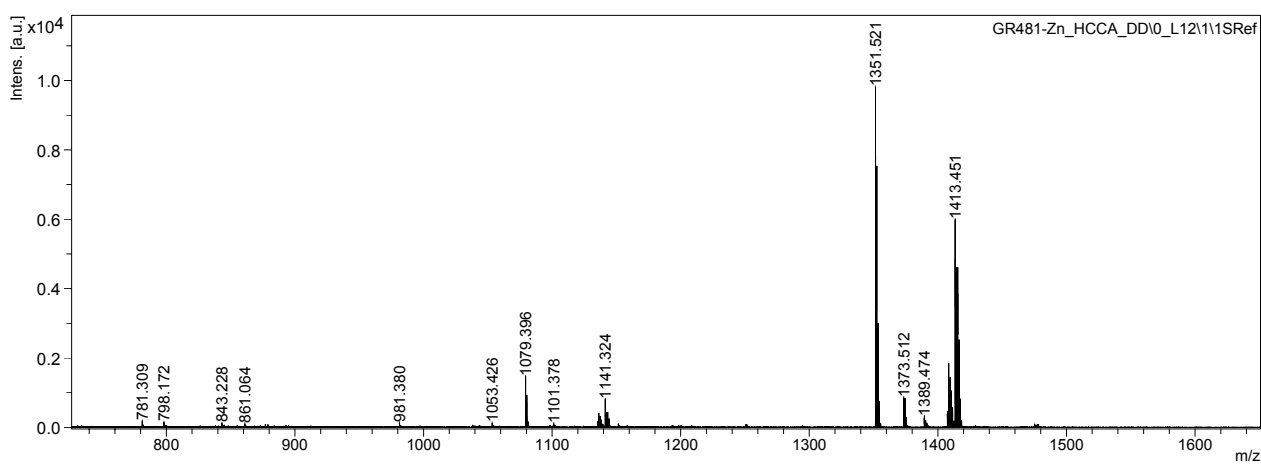
MALDI-TOF ( $m/z$ )  $[\text{M}]^+$  calc for  $\text{C}_{63}\text{FeH}_{71}\text{N}_{19}\text{O}_{15} = 1390.2$ , found = 1389.4

UV ( $\text{H}_2\text{O}$ )  $\lambda_{\text{max}}$ , nm ( $\epsilon$ ): 540 (5325)  $\text{M}^{-1}\text{cm}^{-1}$



MALDI-TOF ( $m/z$ )  $[\text{M}]^+$  calc for  $\text{C}_{60}\text{FeH}_{67}\text{N}_{19}\text{O}_{15} = 1350.1$ , found = 1351.5

UV ( $\text{H}_2\text{O}$ )  $\lambda_{\text{max}}$ , nm ( $\epsilon$ ): 540 (5390)  $\text{M}^{-1}\text{cm}^{-1}$



## UV/Vis Spectrophotometric Titrations

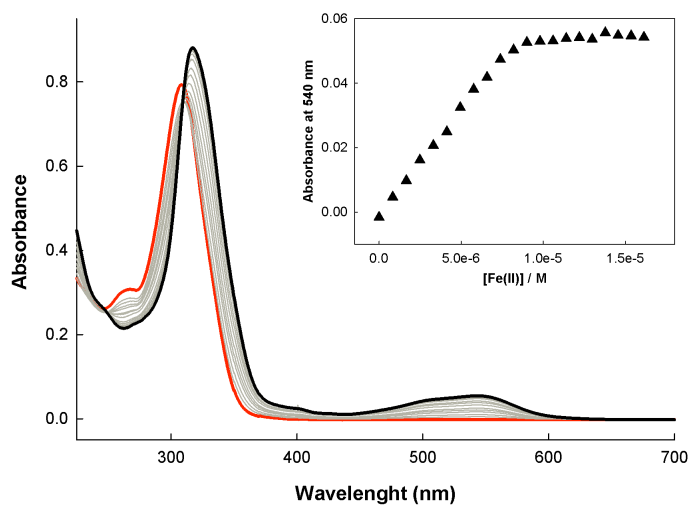


**Figure S1.** Spectrophotometric titration of a  $9.4 \mu\text{M}$  solution of the peptide ligand LL-P in PBS buffer (pH = 5.6) with a standard aqueous solution of Fe(II) ions at 293 K. Inset: titration profile (absorbance vs. concentration of Fe(II) ions) at 540 nm.

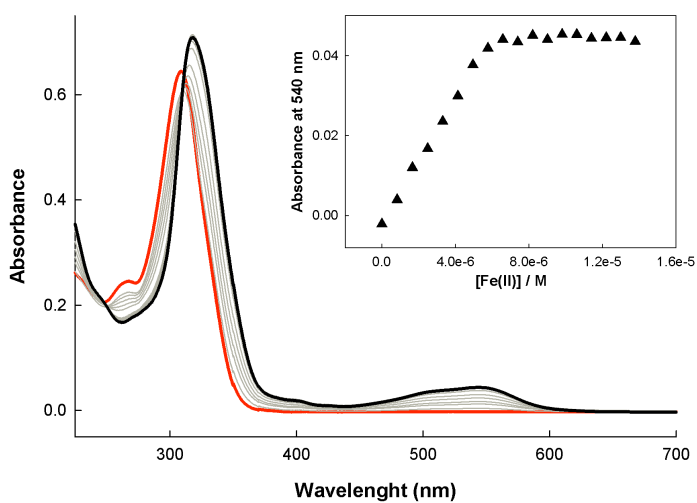


**Figure S2.** Spectrophotometric titration of a  $7.7 \mu\text{M}$  solution of the peptide ligand GL-P in PBS buffer (pH = 5.6) with a standard aqueous solution of Fe(II) ions at 293 K. Inset: titration profile (absorbance vs. concentration of Fe(II) ions) at 540 nm.

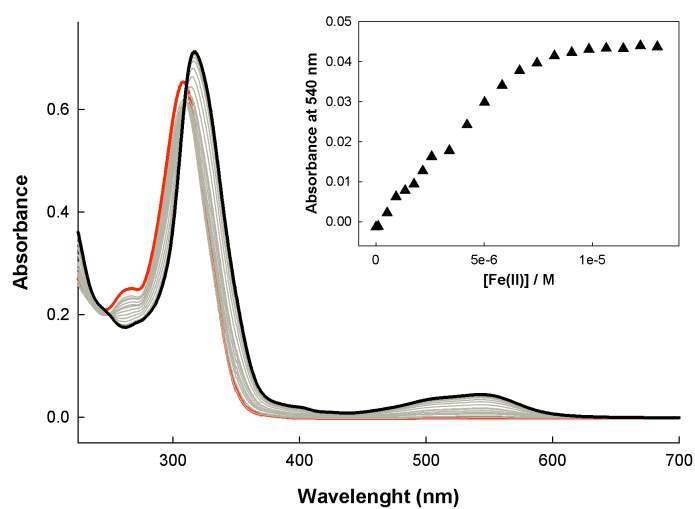


**Figure S3.** Spectrophotometric titration of a 7.6  $\mu\text{M}$  solution of the peptide ligand **DL-P** in PBS buffer (pH = 5.6) with a standard aqueous solution of Fe(II) ions at 293 K. Inset: titration profile (absorbance vs. concentration of Fe(II) ions) at 540 nm.

## Stability Constants of the Fe(II) Tris(bipyridyl) Metallopeptides

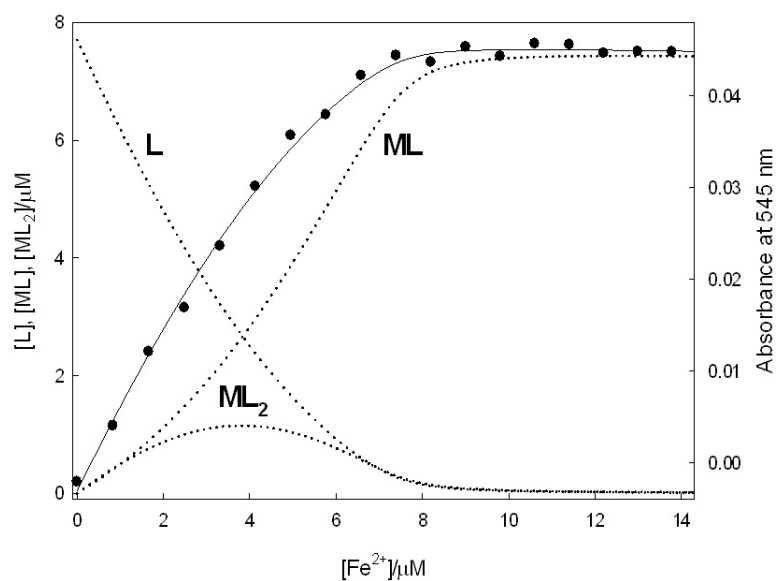


**Figure S4.** UV/Vis titration of 7.7  $\mu\text{M}$  GL-P with increasing concentrations of Fe(II) and best fit to a mixed 1:1 and 1:2 model (solid line). Curves representing the relative populations of free GL-P (L), ML and  $\text{ML}_2$  complexes are overlaid as dashed lines.

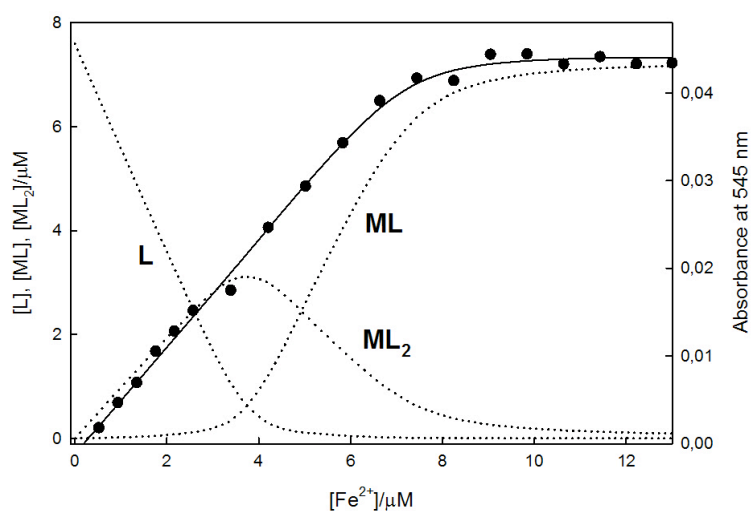


**Figure S5.** UV/Vis titration of 7.6  $\mu\text{M}$  DL-P with increasing concentrations of Fe(II) and best fit to a mixed 1:1 and 1:2 model (solid line). Curves representing the relative populations of free DL-P (L), ML and  $\text{ML}_2$  complexes are overlaid as dashed lines.

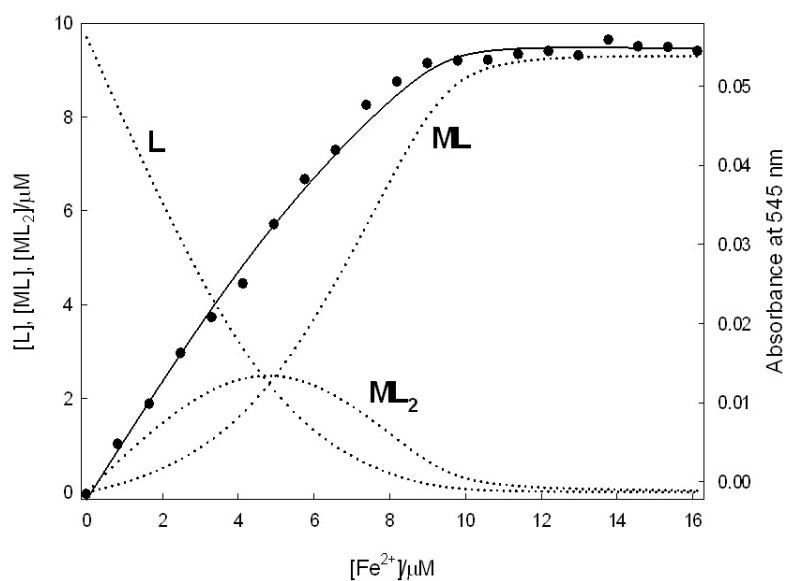


**Figure S6.** UV/Vis titration of 9.4  $\mu\text{M}$  LL-P with increasing concentrations of Fe(II) and best fit to a mixed 1:1 and 1:2 model (solid line). Curves representing the relative populations of free LL-P (L), ML and  $\text{ML}_2$  complexes are overlaid as dashed lines.

**Table S1.** Stability constants of the Fe(II) metallopeptides in PBS at pH 5.6 (293 K).

Metallopeptide	$\log \beta_{1,1}$	$\log \beta_{1,2}$
$[\text{Fe}(\text{LL-P})]^{2+}$	8.01 (0.10)	13.97 (0.19)
$[\text{Fe}(\text{DL-P})]^{2+}$	8.99 (0.12)	16.20 (0.21)
$[\text{Fe}(\text{GL-P})]^{2+}$	7.89 (0.20)	13.13 (0.43)

## CD Spectra of the Fe(II) Tris(bipyridyl) Metallopeptides

Samples contain 400  $\mu\text{L}$  of PBS buffer (10 mM) at pH = 5.01 and 45  $\mu\text{M}$  of the free peptide. The addition of 1 eq. of Fe(II) ions [from a 10 mM solution of  $(\text{NH}_4)\text{Fe}(\text{SO}_4)_2 \cdot 6\text{H}_2\text{O}$  in water] complete the assembly of the corresponding Fe(II) metallopeptide (45  $\mu\text{M}$ ). The spectra are the average of 2 scans. The spectra of the metallopeptides were recorded 250-500 minutes after the addition of the Fe(II) ions. All the spectra were recorded at 293 K.

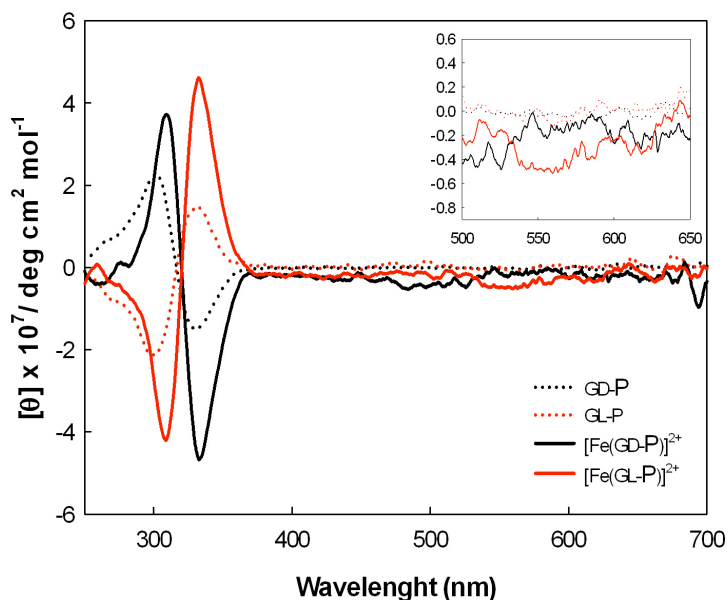


**Figure S7.** CD spectra of GL-P (black dotted line), GL-P (red dotted line),  $[\text{Fe}(\text{GL-P})]^{2+}$  (black solid line) and  $[\text{Fe}(\text{GD-P})]^{2+}$  (red solid line).

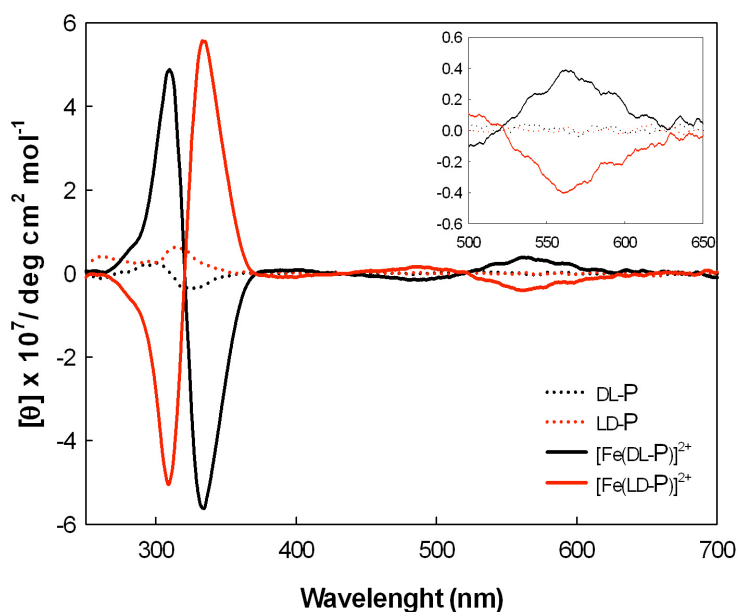


**Figure S8.** CD spectra of LD-P (black dotted line), DL-P (red dotted line),  $[\text{Fe}(\text{LD-P})]^{2+}$  (black solid line) and  $[\text{Fe}(\text{DL-P})]^{2+}$  (red solid line).

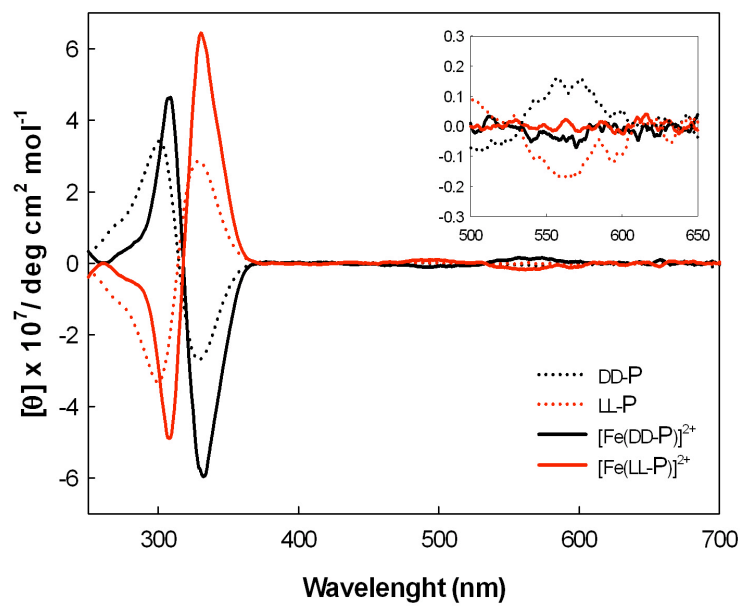


**Figure S9.** CD spectra of LL-P (red dotted line), DD-P (black dotted line), [Fe(LL-P)]<sup>2+</sup> (red solid line) and [Fe(DD-P)]<sup>2+</sup> (black solid line).

## Effect of the Temperature in the Folding Kinetics

*General procedure:* To a thermostated sample of the corresponding free peptide (112  $\mu\text{M}$ ) in 400  $\mu\text{L}$  of PBS buffer (10 mM) at pH = 5.01, 1 eq. of Fe(II) ions was added [from a 10 mM solution of  $(\text{NH}_4)\text{Fe}(\text{SO}_4)_2 \cdot 6\text{H}_2\text{O}$  in water]. The CD spectra of the mixture were recorded every 20 seconds during several hours. The experiment was repeated at 283, 293, 303 and 313 K.

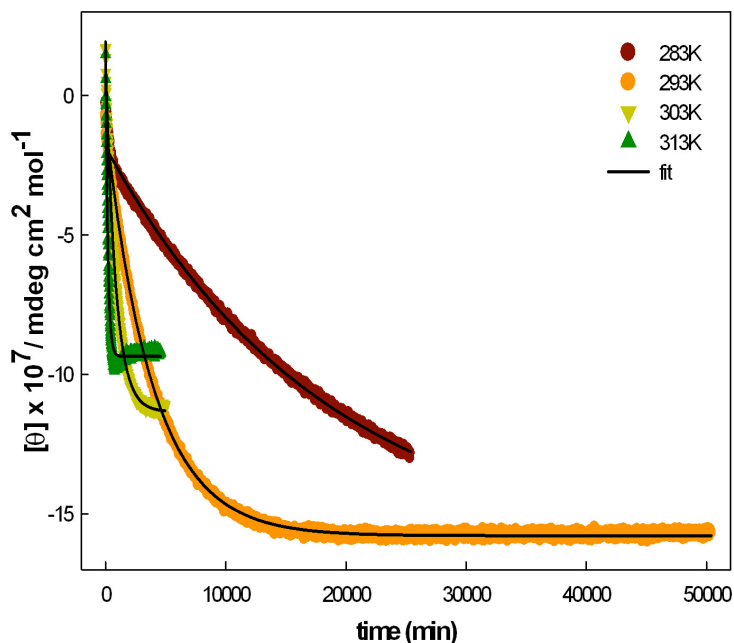


**Figure S10.** Variation of the molar ellipticity of the  $[\text{Fe}(\text{GD-P})]^{2+}$  metallopeptide at 333 nm vs time at 283, 293, 303 and 313 K.

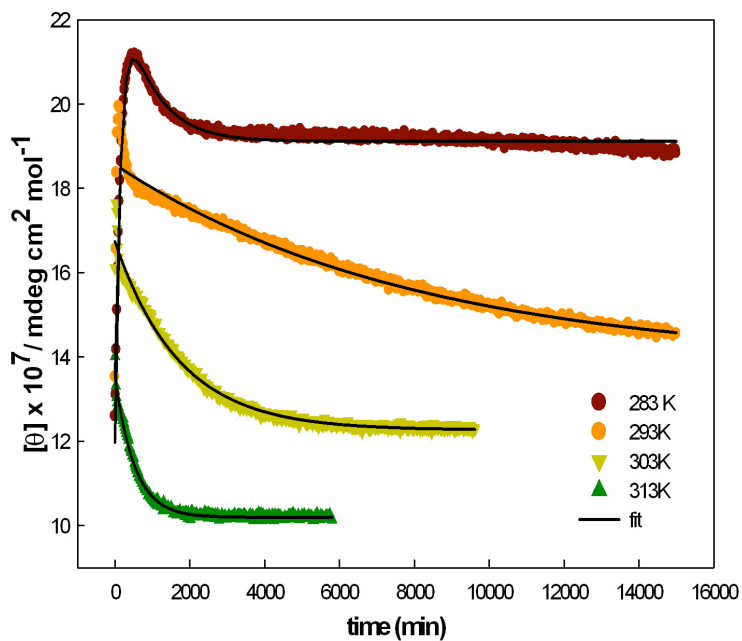


**Figure S11.** Variation of the molar ellipticity of the  $[\text{Fe}(\text{LL-P})]^{2+}$  metallopeptide at 333 nm vs time at 283, 293, 303 and 313 K.

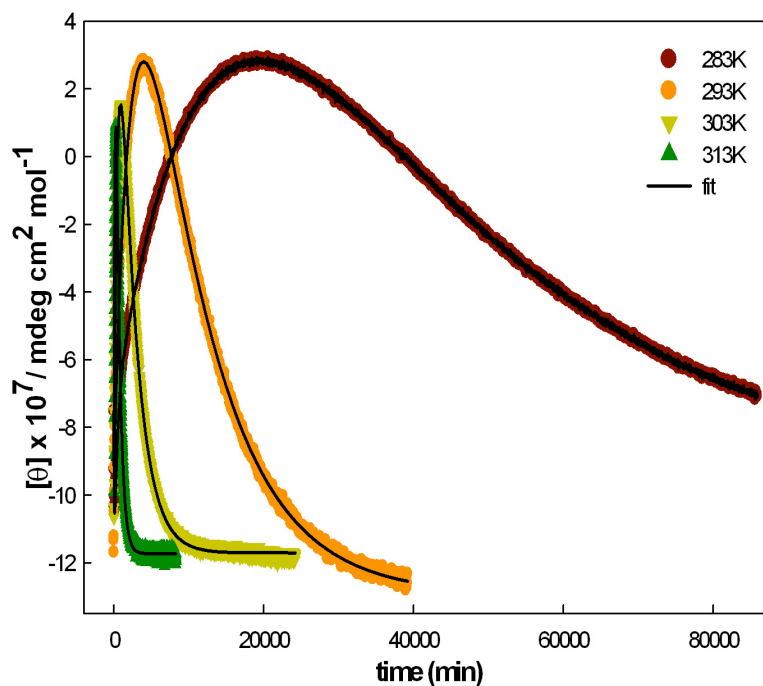


**Figure S12.** Variation of the molar ellipticity of the  $[\text{Fe}(\text{DL-P})]^{2+}$  metallopeptide at 333 nm vs time at 283, 293, 303 and 313 K.

**Table S2.** Folding rate ( $\text{s}^{-1}$ ) extrapolated by applying equations (1) and (2).

T (K)	$[\text{Fe}(\text{GD-P})]^{2+}$	$[\text{Fe}(\text{LL-P})]^{2+}$	$[\text{Fe}(\text{DL-P})]^{2+}$
283	5.412 E-5 (5.9 E-8)	2.099 E-3 (1.3 E-5)	8.539 E-5 (4.9 E-8)
		5.299 E-3 (2.9 E-5)	2.553 E-5 (9.3 E-9)
293	2.566 E-4 (2.4 E-7)	2.849 E-2 (5.6 E-4)	4.018 E-4 (4.1 E-7)
		4.592 E-3 (8.5 E-5)	1.146 E-4 (6.5 E-8)
303	1.200 E-3 (2.5 E-6)	5.834 E-4 (2.9 E-6)	1.987 E-3 (2.7 E-6)
			4.762 E-4 (3.3 E-7)
313	5.634 E-3 (5.8 E-5)	1.736 E-3 (1.9 E-5)	6.510 E-3 (1.1 E-5)
			1.980 E-3 (2.0 E-6)

$$(1) [\theta]_t = [\theta]_\infty + ([\theta]_0 - [\theta]_\infty) e^{-r^*t}$$

$$(2) [\theta]_t = [\theta]_\infty + [e^{-(r1^*t)} + (r1/(r2-r1))] * (e^{-(r1^*t)} - e^{-(r2^*t)}) + (1 - (r2/(r2-r1))) * (e^{-(r1^*t)}) + (r1/(r2-r1)) * (e^{-(r2^*t)})]$$

## Kinetic Studies at Constant Temperature

*General procedure:* To a thermostated sample (313 K) of the corresponding free peptide (at different concentrations) in 400  $\mu\text{L}$  of PBS buffer (10 mM) at pH = 5.01, 1 eq. of Fe(II) ions was added [from a 10 mM solution of  $(\text{NH}_4)\text{Fe}(\text{SO}_4)_2 \cdot 6\text{H}_2\text{O}$  in water]. The CD spectra of the mixture were recorded every 2 minutes during 50 minutes, approximately.

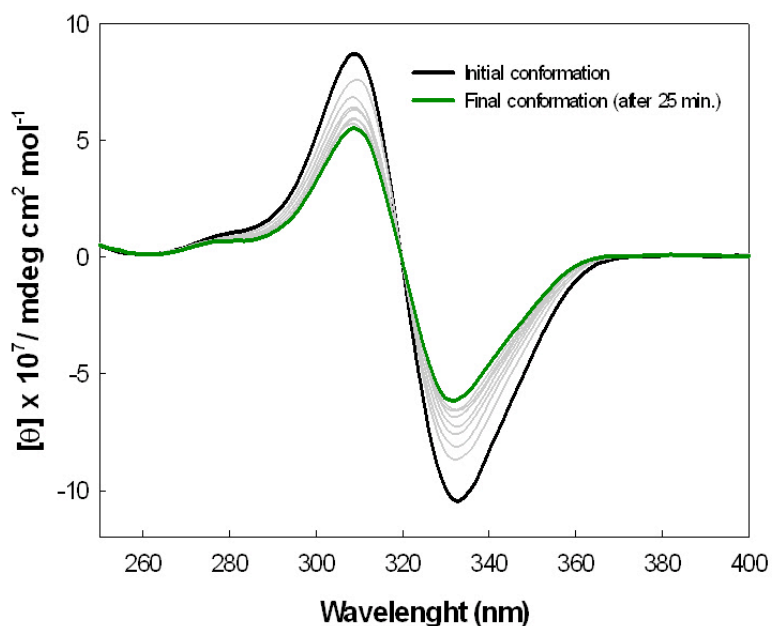


**Figure S13.** CD spectra of the  $[\text{Fe}(\text{DD-P})]^{2+}$  metallopeptide (37  $\mu\text{M}$ ) at 313 K. (2 min between spectra).

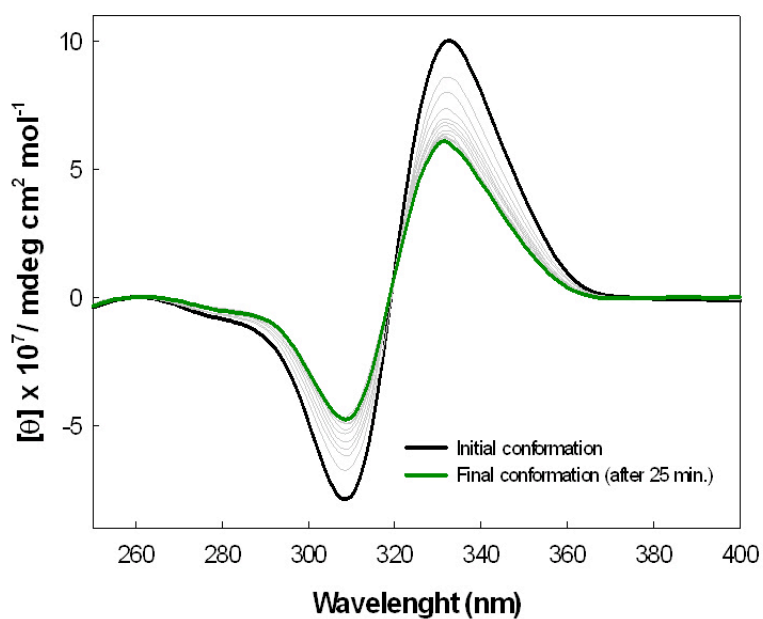


**Figure S14.** CD spectra of the  $[\text{Fe}(\text{LL-P})]^{2+}$  metallopeptide (37  $\mu\text{M}$ ) at 313 K. (2 min between spectra).

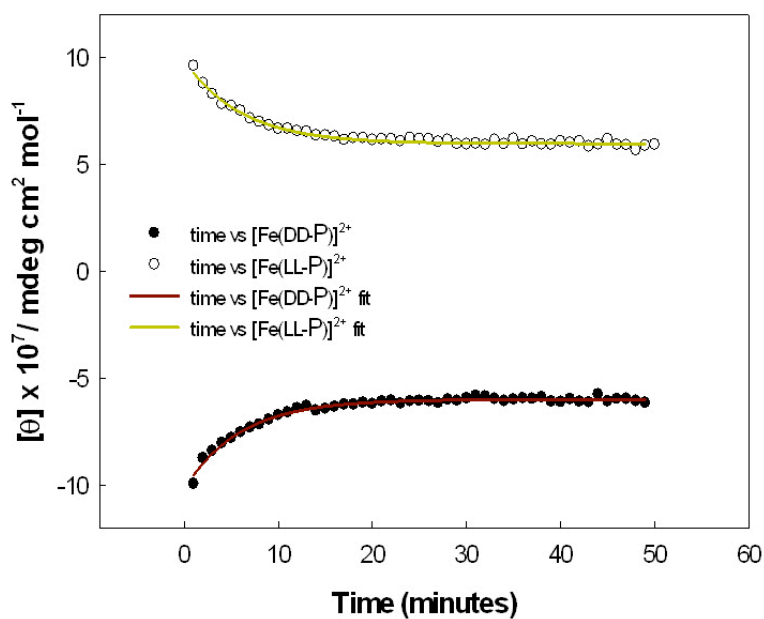


**Figure S15.** Molar ellipticity of the  $[\text{Fe}(\text{DD-P})]^{2+}$  and  $[\text{Fe}(\text{LL-P})]^{2+}$  metallopeptides ( $37 \mu\text{M}$ ) at 332 nm and 313 K (2 min between spectra).

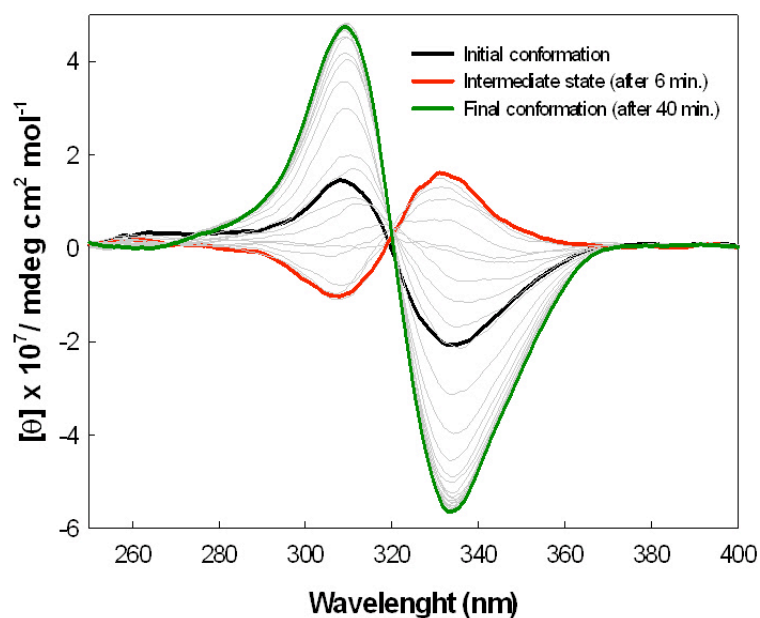


**Figure S16.** CD spectra of the  $[\text{Fe}(\text{DL-P})]^{2+}$  metallopeptide ( $45 \mu\text{M}$ ) at 313 K (2 min between spectra).

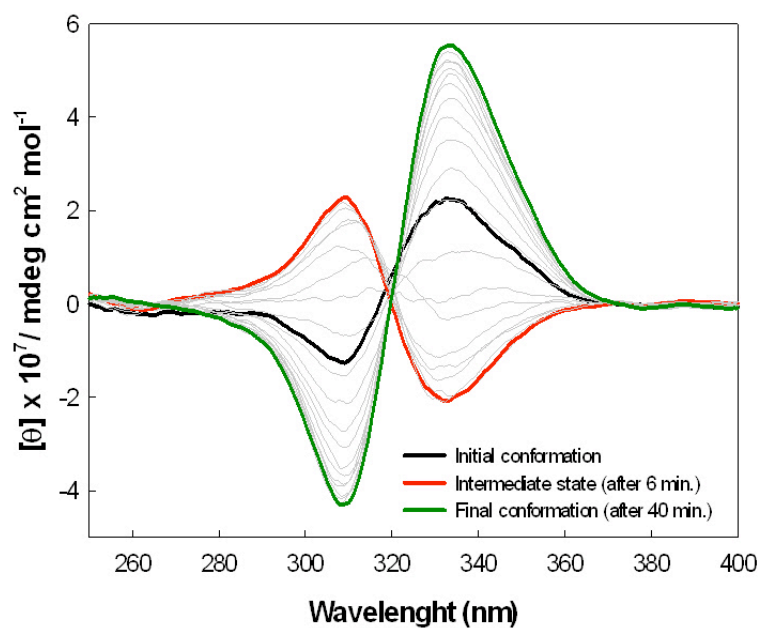


**Figure S17.** CD spectra of the  $[\text{Fe}(\text{LD-P})]^{2+}$  metallopeptide ( $45 \mu\text{M}$ ) at  $313 \text{ K}$  (2 min between spectra).

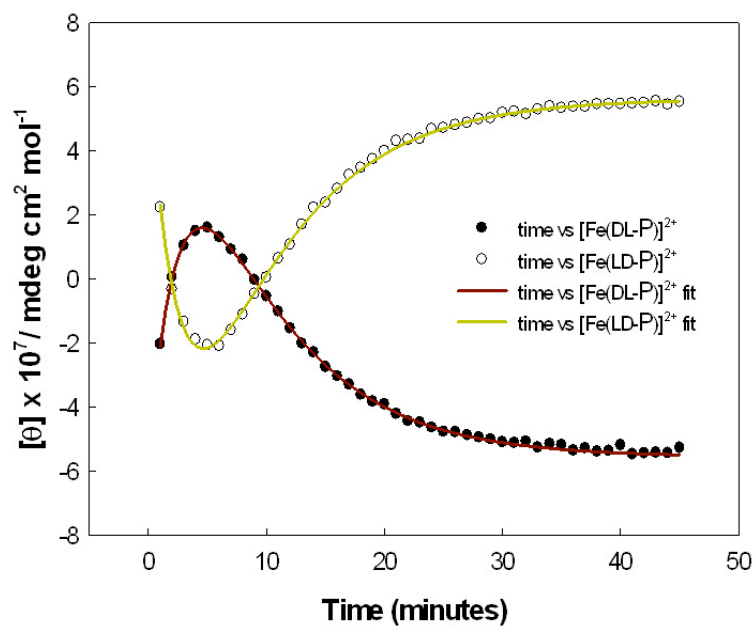


**Figure S18.** Molar ellipticity of the  $[\text{Fe}(\text{DL-P})]^{2+}$  and  $[\text{Fe}(\text{LD-P})]^{2+}$  metallopeptides ( $45 \mu\text{M}$ ) at  $332 \text{ nm}$  and  $313 \text{ K}$  (2 min between spectra).

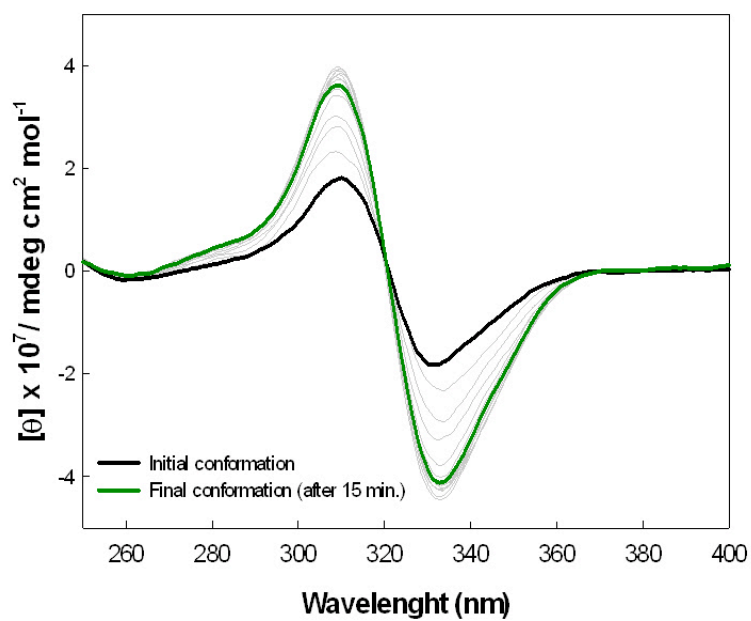


**Figure S19.** CD spectra of the  $[\text{Fe}(\text{GD-P})]^{2+}$  metallopeptide ( $31 \mu\text{M}$ ) at  $313 \text{ K}$  (2 min between spectra).

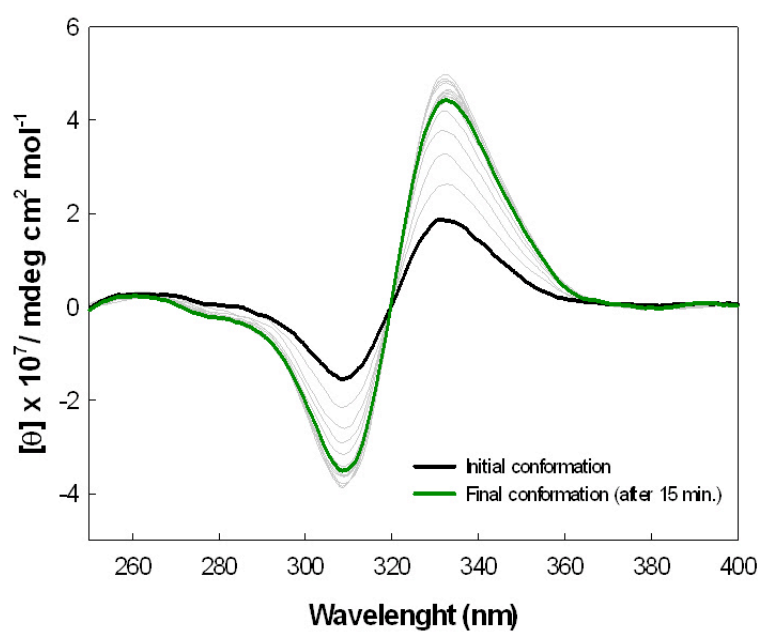


**Figure S20.** CD spectra of the  $[\text{Fe}(\text{GL-P})]^{2+}$  metallopeptide ( $31 \mu\text{M}$ ) at  $313 \text{ K}$  (2 min between spectra).

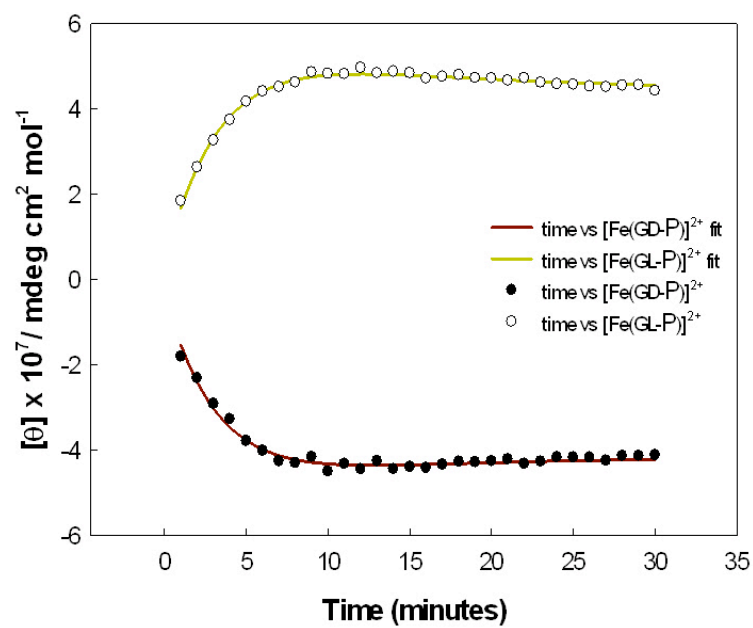


**Figure S21.** Molar ellipticity of the  $[\text{Fe}(\text{GL-P})]^{2+}$  and  $[\text{Fe}(\text{GD-P})]^{2+}$  metallopeptides ( $31 \mu\text{M}$ ) at 332 nm and 313 K (2 min between spectra).

# HPLC

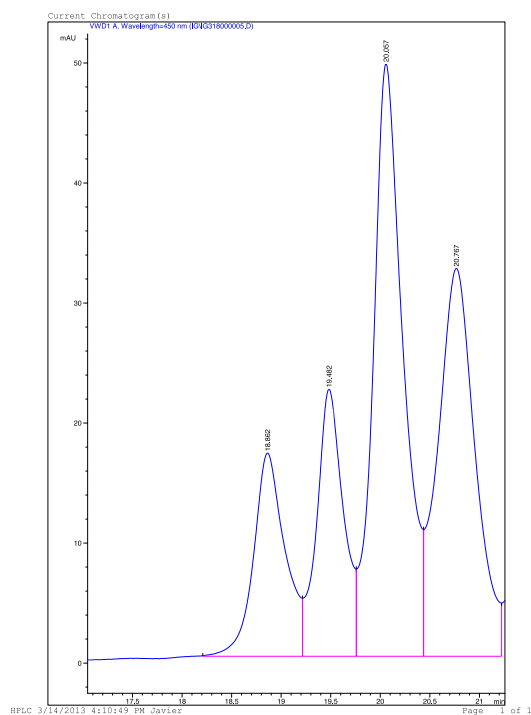


**Figure S22.** HPLC pattern (conditions: isocratic regime 5 % solvent B and 95 % solvent A, during the first 5 min, followed by a linear gradient from 5 % to 25 % of solvent B for 30 min (A: water, B: acetonitrile 0.1% TFA)) of a 0.3 mM aqueous solution of  $[\text{Fe}(\text{DL-P})]^{2+}$  at 298 K. Peaks are noted as A, B, C and D, from left to right. The peaks were collected and immediately lyophilized.

## NMR studies

All NMR experiments were carried out on a Bruker Avance 600 spectrometer operating at 600.13 MHz for  $^1\text{H}$ , 150.90 MHz for  $^{13}\text{C}$ , and 90.56 MHz for  $^2\text{H}$ , equipped with a triple resonance inverse room temperature probe with Z-only gradients.

NMR experiments were done with compound  $[\text{Fe}(\text{LL-P})]^{2+}$ . The typical NMR sample contained  $[\text{Fe}(\text{LL-P})]^{2+}$  (1.5 mM) in 580  $\mu\text{L}$   $\text{D}_2\text{O}$  buffer (10 mM sodium phosphate, pH 5.0, 0.3 mM EDTA) in a 5 mm NMR tube. The solution also contained  $\text{NH}_4^+$  and sulphate ions from the Mohr's salt used to form the complex.

Compound  $[\text{Fe}(\text{LL-P})]^{2+}$  was characterized with 1D ( $^1\text{H}$ ) and 2D (HSQC, COSY, TOCSY, NOESY and ROESY) spectra recorded at temperatures of 278, 298, and 318 K. When required, the resonance of water was suppressed with presaturation or excitation sculpting elements included in the pulse sequences.

Assignment of  $[\text{Fe}(\text{LL-P})]^{2+}$ . Resonances cannot be fully assigned due to the existence of several isomers (4) and severe resonance overlap. Nevertheless, some groups of resonances can be identified in the aromatic region with the aid of 1D- $^1\text{H}$  and 2D spectra. The partial assignment of the aromatic protons is shown in figure S25 and is deduced from the following observations.

1. The complexity of the aromatic  $^1\text{H}$  region indicates that there are several isomers of  $[\text{Fe}(\text{LL-P})]^{2+}$ . A single isomer has only 18 aromatic H (3 Bpy moieties, with 6 H each) [Figures S23 and S24].
2. Aromatic  $^1\text{H}$  resonances are grouped in several bands containing signals of similar shape and multiplicity: **A** ( $\delta_{\text{H}} = 7.5 - 7.8$  ppm), **B** ( $\delta_{\text{H}} = 7.8 - 8.1$  ppm), **C** ( $\delta_{\text{H}} = 8.1 - 8.2$  ppm), **D** ( $\delta_{\text{H}} = 8.2 - 8.4$  ppm), **E** ( $\delta_{\text{H}} = 8.45 - 8.55$  ppm) [Figure S23]. Protons in each band are of the same type, as evidenced by their similar  $\delta_{\text{C}}$  in the HSQC ( $\delta_{\text{C}}$ : **A**  $\approx 153$  ppm, **B**  $\approx 145$  and 129 ppm, **C**  $\approx 145$  ppm, **D**  $\approx 137$ , **E**  $\approx 123 - 125$  ppm) [Figure S28].
3. Doublets in band **A** ( $\delta_{\text{H}} = 7.5 - 7.8$  ppm) have a small coupling of  $^4J_{\text{H3-H5}} \approx 1.8$  Hz, hence they are assigned to the H3 protons [Figure S24].
4. Taking into account that each molecule of  $[\text{Fe}(\text{LL-P})]^{2+}$  has three Bpy rings (hence  $3 \times \text{H3}$  and  $3 \times \text{H3}'$  resonances), this group of  $12 \times \text{H3}$  resonances in region **A** ( $\delta_{\text{H}} = 7.5 - 7.8$  ppm) indicates that there are four species (isomers) in the mixture. Integral values match approximately with 72 aromatic protons, in agreement with the existence of four isomers. Note from the intensities of the H3 resonances that the four isomers are approximately equimolecular [Figure S24].
5. Bands **B** ( $\delta_{\text{H}} = 7.8 - 8.1$  ppm) and **C** ( $\delta_{\text{H}} = 8.1 - 8.2$  ppm) contain protons that can be assigned to H5 and H5' due to their multiplicity (*dd* with one small and one large coupling:  $^4J_{\text{H3-H5}} \approx 1.9$  Hz,  $^3J_{\text{H5-H6}} \approx 8$  Hz) [Figure S24].
6. The H6 and H6' resonances are grouped in band **E** ( $\delta_{\text{H}} = 8.45 - 8.55$  ppm); there are no H6 or H6' resonances in bands **B** or **C**. This is clearly seen in the TOCSY spectrum, which shows cross-peaks between bands **B/E** and **D/E**, ( $\text{H5}'/\text{H6}'$  and  $\text{H5}/\text{H6}$   $^3J_{\text{HH}}$  correlations) but not between resonances belonging to the same band **B** or **D** [Figure S26]. Values of  $\delta_{\text{C}}$  in the HSQC support this conclusion [Figure S28].
7. Band **B** ( $\delta_{\text{H}} = 7.8 - 8.1$  ppm) contains the 12 H5', and band **D** ( $\delta_{\text{H}} = 8.2 - 8.4$  ppm) contains the 12 H5. This is deduced from the COSY weak correlations due to the small  $^4J_{\text{H3-H5}}$  couplings: (i) between

bands **A** (H3,  $\delta_{\text{H}} = 7.5 - 7.8$  ppm) and **D** (H5,  $\delta_{\text{H}} = 8.2 - 8.4$  ppm); and (ii) between bands **C** (H3',  $\delta_{\text{H}} = 8.1 - 8.2$  ppm) and **B** (H5',  $\delta_{\text{H}} = 7.8 - 8.1$  ppm) [Figure S25].

8. Band **B** ( $\delta_{\text{H}} = 7.8 - 8.1$  ppm) also contains 9 H3' resonances overlapped with the H5' resonances. This is deduced from the  $^1\text{H}$  integral [Figure S24], from the HSQC (which shows two types of H with distinct  $\delta_{\text{C}} \approx 129$  and 145 ppm) [Figure S28], and from the weak COSY cross-peaks between resonances within band **B** (which are due to the small coupling  $^4J_{\text{H3'-H5'}}$ ) [Figure S25].

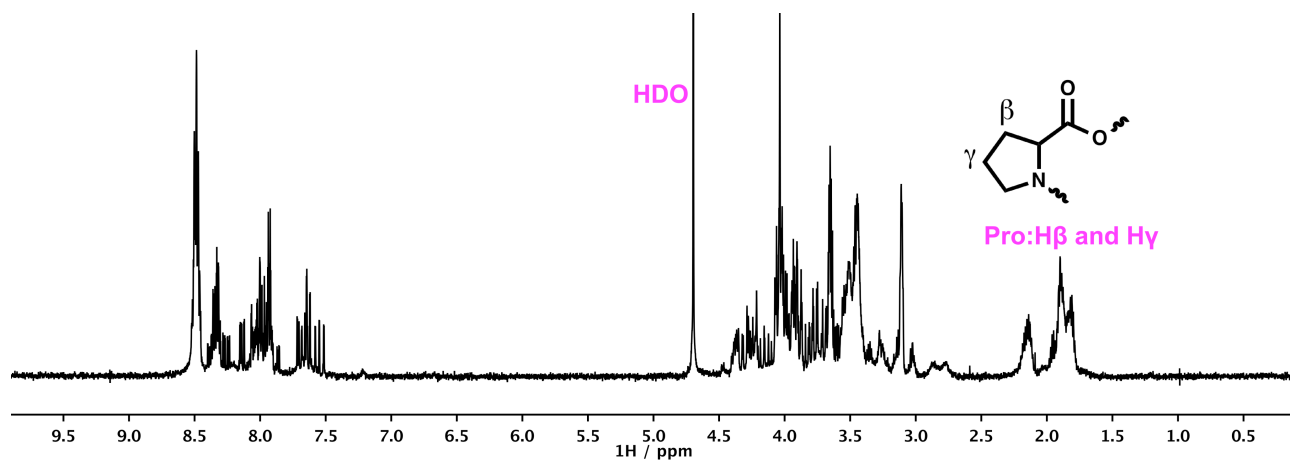


**Figure S23.**  $^1\text{H}$ -NMR (600 MHz, 298 K) spectrum of compound  $[\text{Fe}(\text{LL-P})]^{2+}$  (1.5 mM) in  $\text{D}_2\text{O}$  buffer.

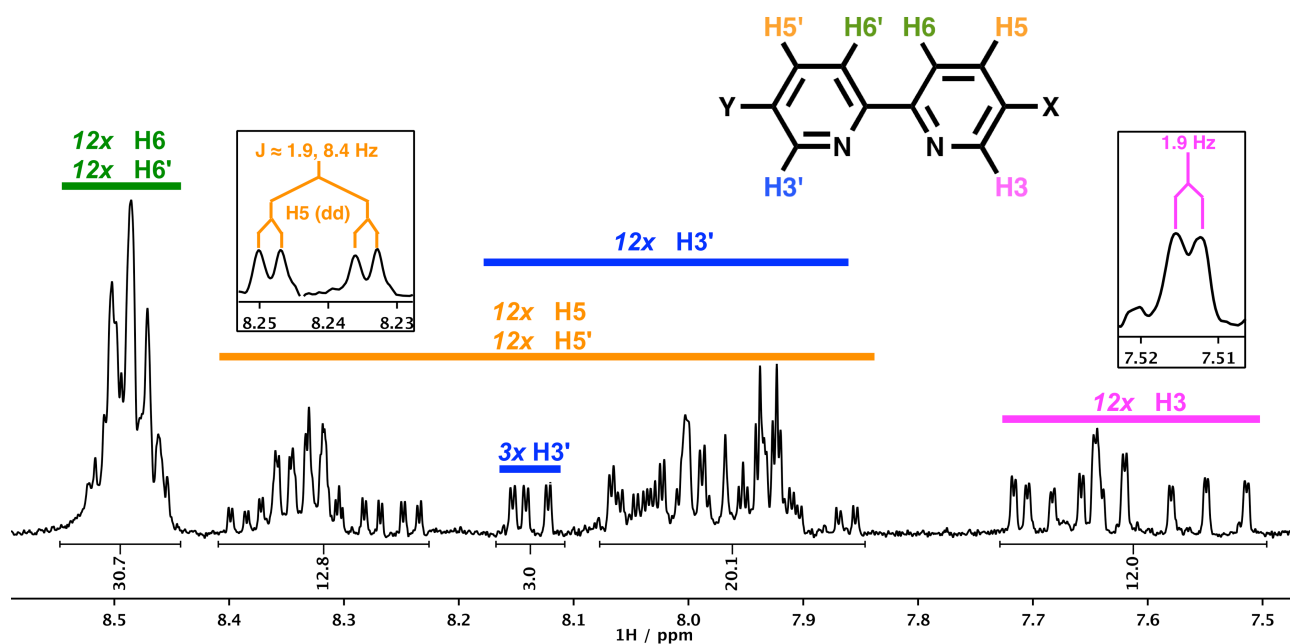


**Figure S24.** Expansion of the aromatic region of spectrum S1. The insets show representative multiplets from the aromatic region of spectrum S1. Peak multiplicities and scalar coupling values are used to identify the H3/3' and H5/5' resonances. Doublets in the region  $\delta_{\text{H}} = 7.5 - 7.8$  ppm have a small coupling  $^4J_{\text{H}_3-\text{H}_5} \approx 1.8 - 2.0$  Hz, hence they are assigned to the H3 protons (*magenta*). Resonances appearing as doublet of doublets (*dd*) with one small and one large coupling ( $^4J_{\text{H}_3-\text{H}_5} \approx 1.9$  Hz,  $^3J_{\text{H}_5-\text{H}_6} \approx 8$  Hz) correspond to H5/H5' protons (*orange*). This is further confirmed in the TOCSY spectrum as H5/H5' correlate with H6/H6' protons at  $\delta_{\text{H}} = 8.45 - 8.55$  ppm (*green*), while H3 protons do not correlate with any other protons. Taking into account that each molecule of  $[\text{Fe}(\text{LL-P})]^{2+}$  has three Bpy rings (hence  $3 \times$  H3 resonances), this group of  $12 \times$  H3 resonances in the 7.5–7.8 ppm region indicates that there are four species in the mixture.

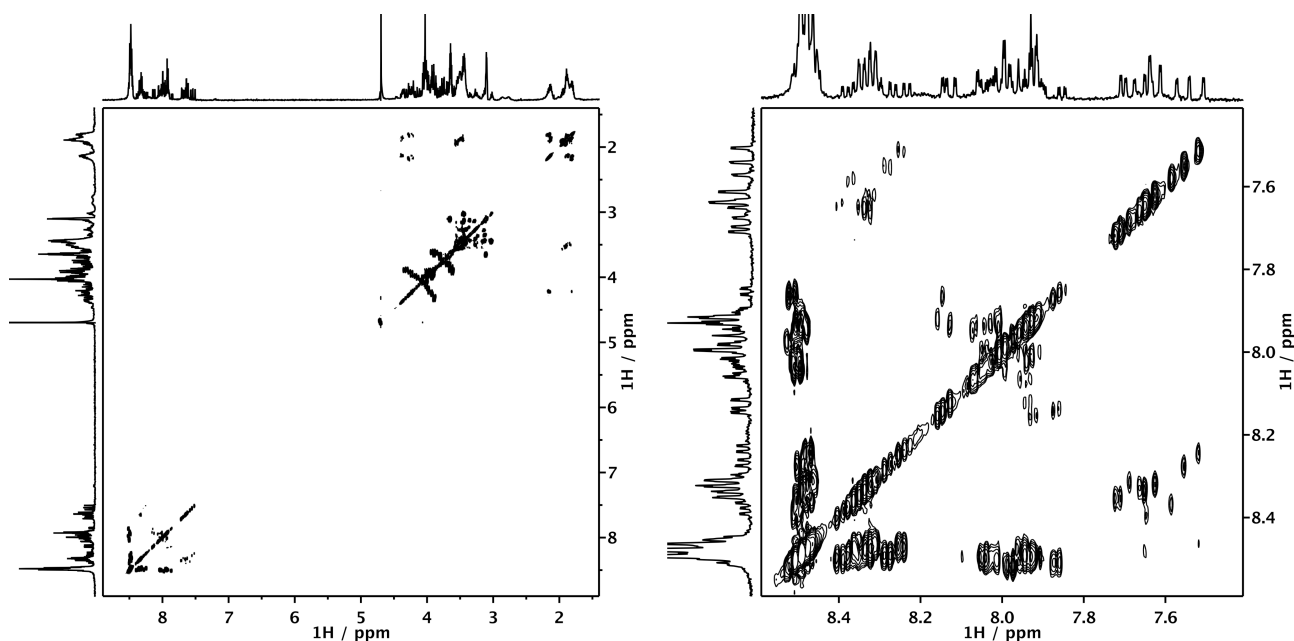


**Figure S25.** COSY spectrum of  $[\text{Fe}(\text{LL-P})]^{2+}$  (600 MHz, 298 K). *Left*, full spectrum; *right*, expansion of the aromatic region. Cross-peaks in the aromatic region support the assignment of groups of resonances to H3/3', H5/5' and H6/6' protons of the Bpy rings. Note (i) the strong cross-peaks H5/H6 and H5'/H6' ( ${}^3J_{\text{HH}}$ ); (ii) the weaker cross-peaks H3/H5 and H3'/H5' ( ${}^4J_{\text{HH}}$ ); and (iii) the absence of correlations H3/H6 and H3'/H6'.

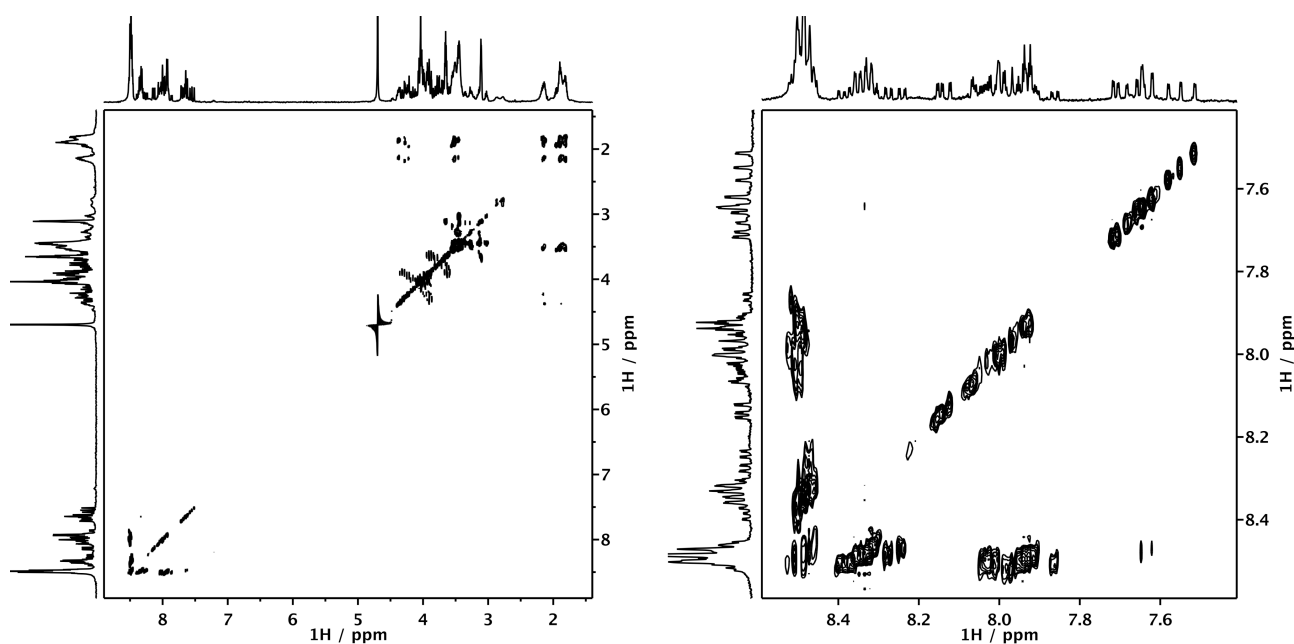


**Figure S26.** TOCSY spectrum of  $[\text{Fe}(\text{LL-P})]^{2+}$  recorded with 60 ms mixing time (600 MHz, 298 K). *Left*, full spectrum; *right*, expansion of the aromatic region. Cross-peaks in the aromatic region support the assignment of groups or resonances to H3, H5 and H6 protons of the Bpy rings. Note the correlation of H5/H5' with H6/H6' protons, and the absence of correlations of H3 and H3' protons.

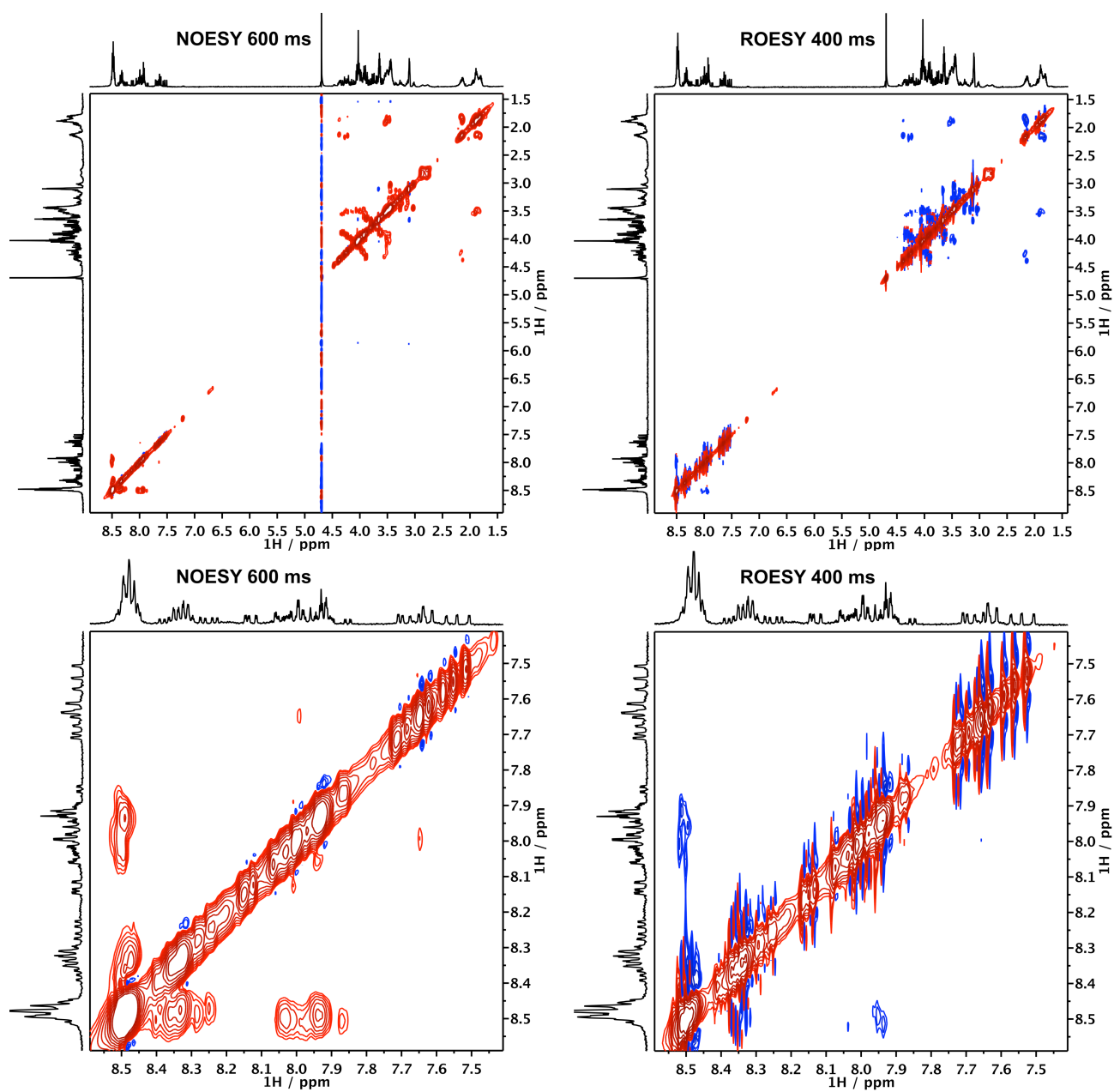


**Figure S27.** NOESY (left,  $t_{\text{mix}} = 600$  ms) and ROESY (right,  $t_{\text{mix}} = 400$  ms) spectra of  $[\text{Fe}(\text{LL-P})]^{2+}$  (600 MHz, 298 K). Top, full spectrum; bottom, expansion of the aromatic region.

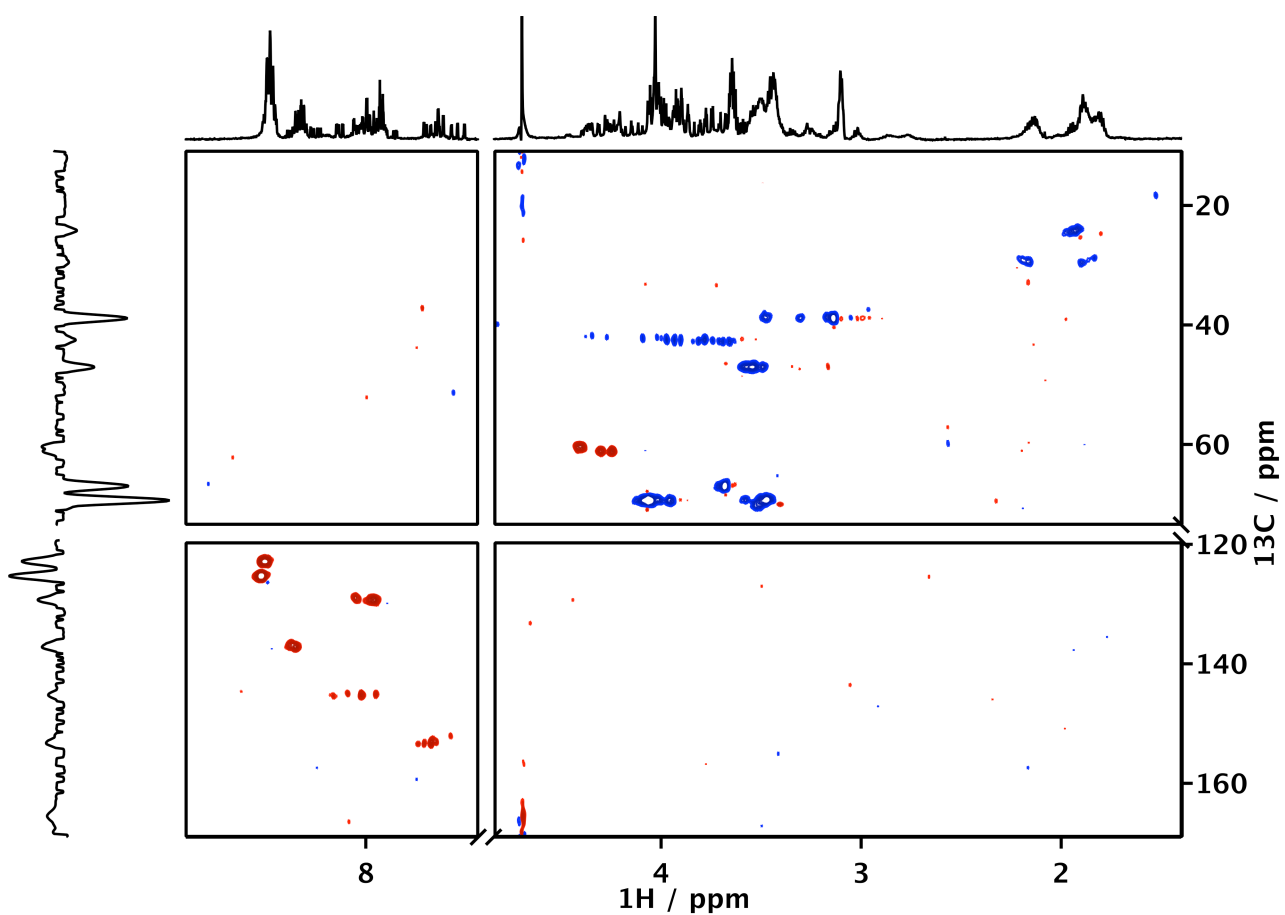


**Figure S28.** Multiplicity-edited HSQC spectrum of  $[\text{Fe}(\text{LL-P})]^{2+}$  (600 MHz, 298 K). Peak sign is colour-coded: *red*, positive (CH and CH<sub>3</sub>); *blue*, negative (CH<sub>2</sub>). Each type of aromatic CH in the Bpy ring has a narrow range of  $\delta_{\text{C}}$  that aids in the assignment of the  $^1\text{H}$  spectrum.

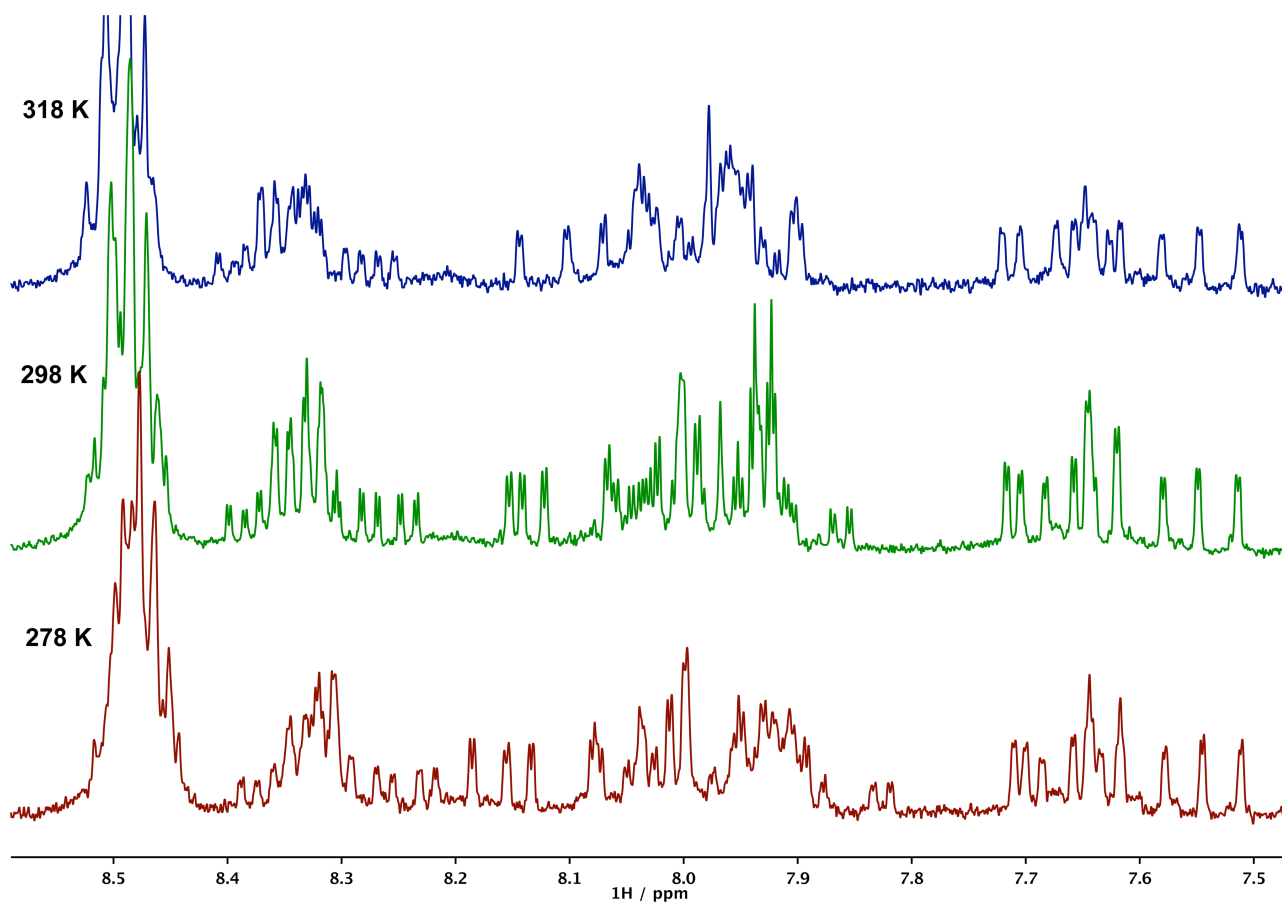


**Figure S29.** Variable-temperature NMR of compound  $[\text{Fe}(\text{LL-P})]^{2+}$  at 600 MHz. Expansion of the aromatic region. Temperatures: 278 K (*brown*), 298 K (*green*), and 318 K (*blue*). There is no sign of interconversion of species upon heating, indicating that chemical exchange is in the slow regime in the chemical shift timescale. [Note that the HPLC and CD experiments demonstrated that these four isomers interconvert].

## Molecular Modeling Studies

Two types of modeling were performed in this study and carried out both on the isolated ligand and all the  $[\text{Fe}(\text{XX-P})]^{2+}$  complexes were ( $X$  are L or D-Pro). The most complex exercise was the latter as it concentrated on generating 3D models of the metal bound peptides. To do so, an initial set of  $[\text{Fe}(\text{XX-P})]^{2+}$  structures was generated in such a way that all the coordination sites of the metal were occupied by nitrogen atoms from the bipyridine rings. This exploration showed that two successive bipyridine rings can only be *cis* one with respect to the other. Despite the length of the loop, no *trans* geometries are structurally allowed. Using both UCSF Chimera (ref UCSF Chimera) and Gaussview molecular visualization and building tools, a total of 10 physically sound structures with different chirality (5  $\Lambda$  and 5  $\Delta$ ) were generated. On each, QM/MM calculations were performed using the ONIOM scheme (ref ONIOM) implemented in the Gaussian09 (ref Gaussian). Calculations were performed using the (B3LYP:AMBER)(ref B3LYP, ref AMBER) with a mixed basis set for the quantum mechanical region corresponding to the aug-cc-pVTZ basis set for the metal (ref aug-cc-pVTZ) and the 6-311G\* for the other atoms (ref 6-311G\*). Parameters for the MM region were obtained with the GAFF force field throughout the Antechamber interface integrated in UCSF Chimera (ref GAFF). The QM region of this system was limited to the iron and the entire bipyridine rings using and hydrogen atom as linker. Geometry optimizations were first undertaken in gas phase with mechanical embedding. After this initial relaxation of the systems, they were re-optimized including solvent effect with the CPCM model simulating the water conditions (ref CPCM) and electronic embedding. On these systems, the calculation of the dispersion energy was added using Grimme's approach D3 (ref D3) available on the web page (<http://www.tch.uni-bonn.de/>)

Molecular Dynamics simulations were performed on the isolated ligands. The objective of this part of the work was to study the amount of preorganization of the peptide on the metal binding process as well as identify possible trends on the formation of the loops and any implication of the chirality of the proline residues. Calculations were performed with the MMTK MD (ref MMTK) driver and under the interface generated by our group in the UCSF Chimera framework (available from download at the same UCSF website). The ligand was prepared with the GAFF force field and the charges associated were calculated with the Gasteiger model. Calculations were undertaken up to 1ns which, based on the small size of the system, already provides with a good sampling. Calculations were carried out in gas phase with no cutoff on none bonding interactions and using the berendsen thermostat. No restriction were applied on the system and statistics performed with the interface of the Molecular Dynamics plug-in of UCSF Chimera.

### *UCSF Chimera*

Pettersen EF, Goddard TD, Huang CC, Couch GS, Greenblatt DM, Meng EC, Ferrin TE. J Comput Chem. 2004, 25, 13, 1605-1612.

### *ONIOM*

Svensson, M.; Humbel, S.; Froese, R. D.; Matsubara, T.; Sieber, S.; Morokuma, K. J. Chem. Phys. 1996, 100, 19357-19363.

### *Gaussian*

Frisch, M. J. Trucks, G. W. Schlegel, H. B. Scuseria, G. E. Robb, M. A. Cheeseman, J. R. Montgomery, J. A. Vreven, Jr., T. Kudin, K. N. Burant, J. C. Millam, J. M. Iyengar, S. S. Tomasi, J. Barone, V. Mennucci, B. Cossi, M. Scalmani, G. Rega, N. Petersson, G. A. Nakatsuji, H. Hada, M. Ehara, M. Toyota, K. Fukuda, R. Hasegawa, J. Ishida, M. Nakajima, T. Honda, Y. Kitao, O. Nakai, H. Klene, M. Li, X. Knox, J. E. Hratchian, H. P. Cross, J. B. Bakken, V. Adamo, C. Jaramillo, J. Gomperts, R. Stratmann, R. E. Yazyev, O. Austin, A. J. Cammi, R. Pomelli, C. Ochterski, J. Ayala, P. Y. Morokuma, K. Voth, G. A. Salvador, P. Dannenberg, J. J. Zakrzewski, V. G. Dapprich, S. Daniels, A. D. Strain, M. C. Farkas, O. Malick, D. K. Rabuck, A. D. Raghavachari, K. Foresman, J. B. Ortiz, J. V. Cui, Q. Baboul, A. G. Clifford, S. Cioslowski, J. Stefanov, B. B. Liu, G. Liashenko, A. Piskorz, P. Komaromi, I. Martin, R. L. Fox, D. J. Keith, T. Al-Laham, M. A. Peng, C. Y. Nanayakkara, A. Challacombe, M. Gill, P. M. W. Johnson, B. G. Chen, W. Wong, M. W. C., G.; Pople, J. A. Gaussian09 Revision D.01, Gaussian Inc. Wallingford CT 2009.

### *B3LYP*

A.D. Becke, J.Chem.Phys. 98 (1993) 5648-5652

C. Lee, W. Yang, R.G. Parr, Phys. Rev. B 37 (1988) 785-789

S.H. Vosko, L. Wilk, M. Nusair, Can. J. Phys. 58 (1980) 1200-1211

P.J. Stephens, F.J. Devlin, C.F. Chabalowski, M.J. Frisch, J.Phys.Chem. 98 (1994) 11623-11627

### *Amber*

Wang, J., Wang, W., Kollman P. A.; Case, D. A. "Automatic atom type and bond type perception in molecular mechanical calculations". Journal of Molecular Graphics and Modelling , 25, 2006, 247260.

### *aug-cc-pVTZ*

Kendall, R. A.; Dunning Jr, T. H.; Harrison, R. J. J. Chem. Phys. 1992, 96, 6796-6806.

Woon, D. E.; Dunning Jr, T. H. J. Chem. Phys. 1993, 98, 1358-1371.

### *6-311G\**

McLean, A.; Chandler, G. J. Chem. Phys. 1980, 72, 5639-5648.

Krishnan, R.; Binkley, J. S.; Seeger, R.; Pople, J. A. J. Chem. Phys. 1980, 72, 650-654.

### *GAFF*

Wang, J., Wolf, R. M.; Caldwell, J. W.;Kollman, P. A.; Case, D. A. "Development and testing of a general AMBER force field". Journal of Computational Chemistry, 25, 2004, 1157-1174.

### *CPCM*

Barone, V.; Cossi, M. J. Phys. Chem. A 1998, 102, 1995-2001.

Cossi, M.; Rega, N.; Scalmani, G.; Barone, V. J. Comput. Chem. 2003, 24, 669-681.

*D3*

Stefan Grimme, Jens Antony, Stephan Ehrlich, and Helge Krieg J. Chem. Phys. 2010, 132, 154104

*MMTK*

Hinsen K. J. Comp. Chem. 2000, 21, 79-85

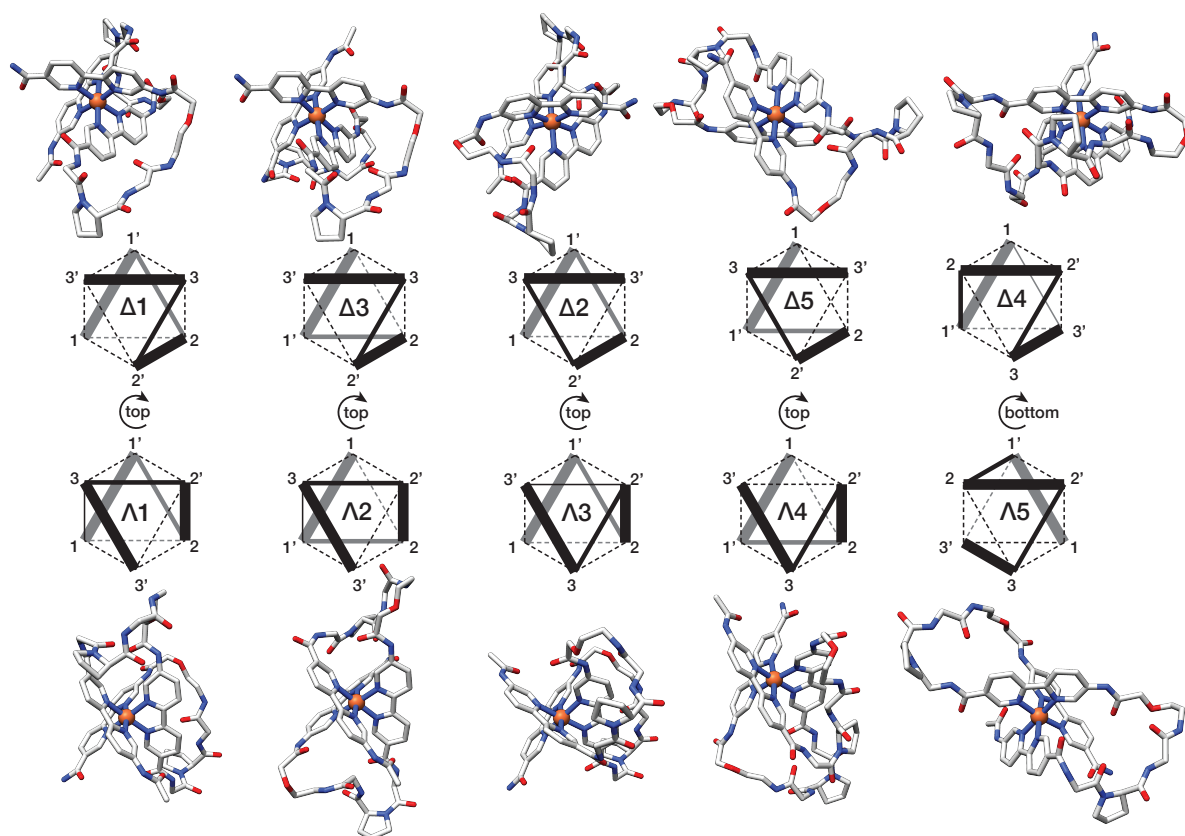


**Figure S30.** The possible isomers of the  $[\text{Fe}(\text{DL-P})]^{2+}$  metallopeptide, as well as their interconversion through twist mechanism. Thick solid lines represent the bipyridines; solid lines represent the linkers between the coordinating O1Pen residues, and the transformation leading to the interconversion is also shown between the different pairs. The proposed structures of each of the isomers are also shown.

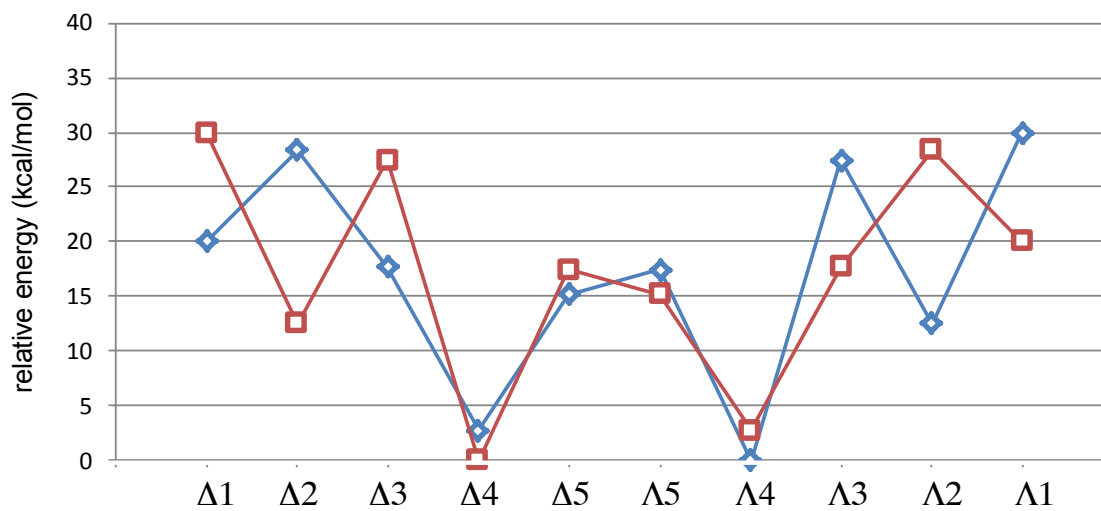


**Figure S31.** QM/MM relative energies for the  $[\text{Fe}(\text{DD-P})]^{2+}$  (blue) and  $[\text{Fe}(\text{LL-P})]^{2+}$  (red) complexes.

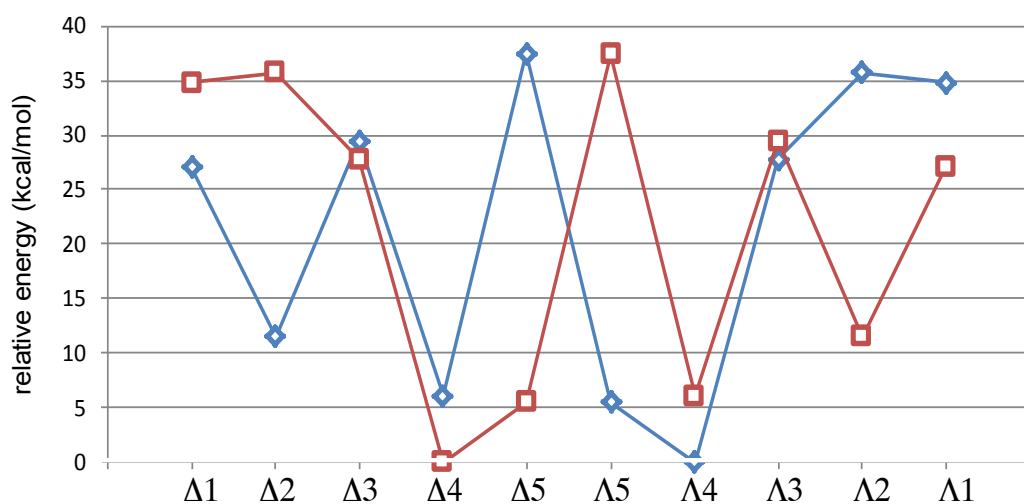


**Figure S32.** QM/MM relative energies for the [Fe(DL-P)]<sup>2+</sup> (red) and [Fe(LD-P)]<sup>2+</sup> (blue) complexes.

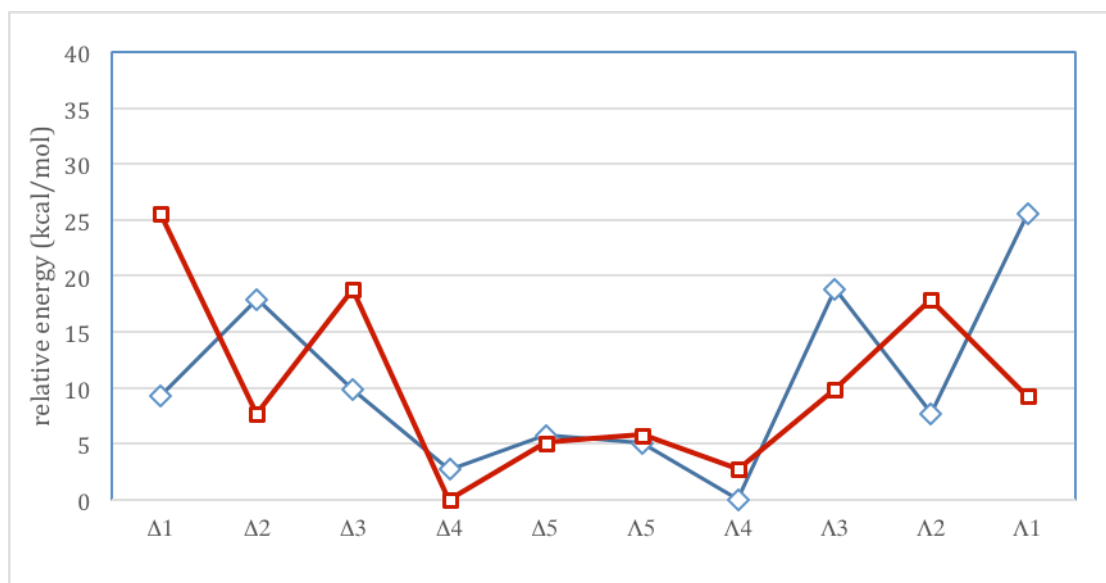


**Figure S33.** QM/MM relative energies for the [Fe(GD-P)]<sup>2+</sup> (blue) and [Fe(GL-P)]<sup>2+</sup> (red) complexes.

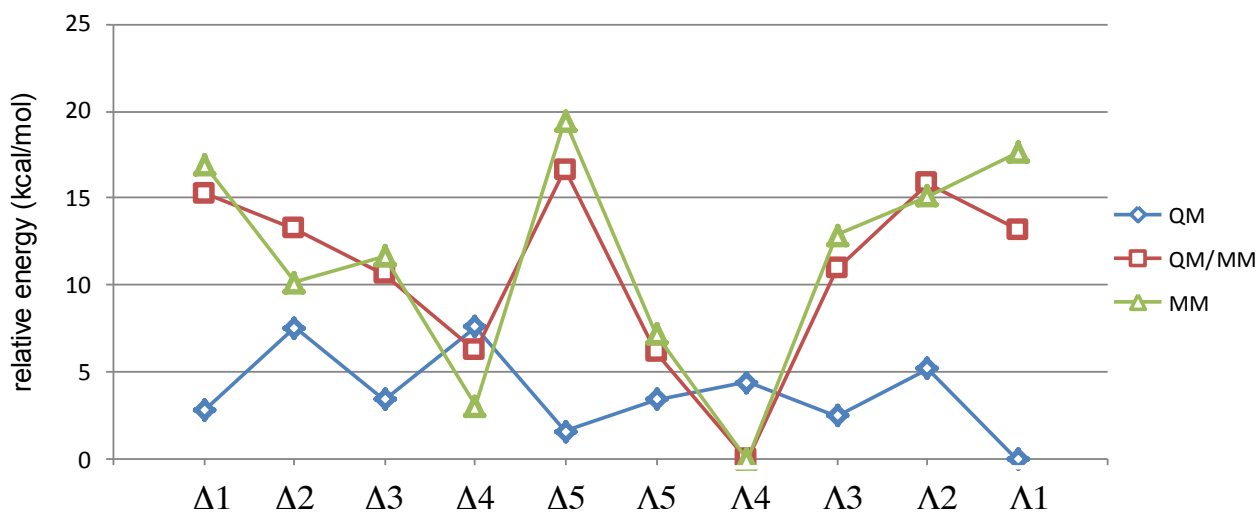


**Figure S34.** QM/MM energy breakdown on its QM and MM terms for the  $[\text{Fe}(\text{LD-P})]^{2+}$  complexes.

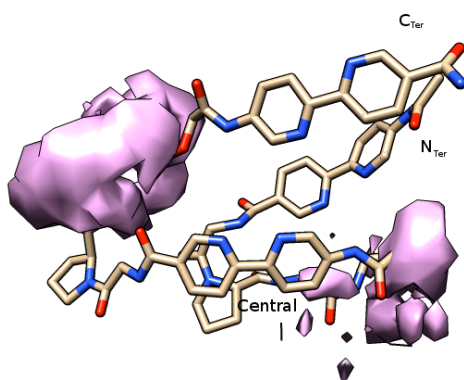


**Figure S35.** Representation of the atomic fluctuations of  $\text{N}_{\text{Ter}}$  and  $\text{C}_{\text{Ter}}$  loops in term of occupancy of nitrogen atom positions. The central,  $\text{N}_{\text{Ter}}$  and  $\text{C}_{\text{Ter}}$  bipyridine rings are indicated for clarity.

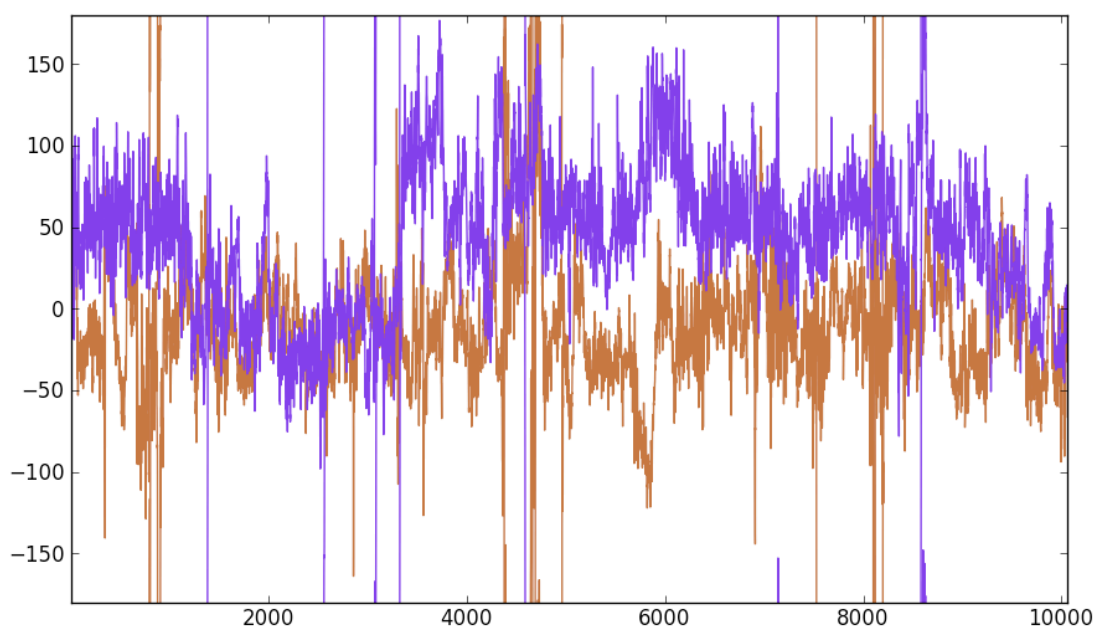


**Figure S36. Analysis of the flexibility of the loops during a MD experiment.** The dihedral angle of four nitrogen atoms of the CTer and NTer loop is used as a marker of the evolution during the 1ns experiment for the **DD-P** ligand. The red and violet graphs correspond to the NTer and CTer loop respectively.

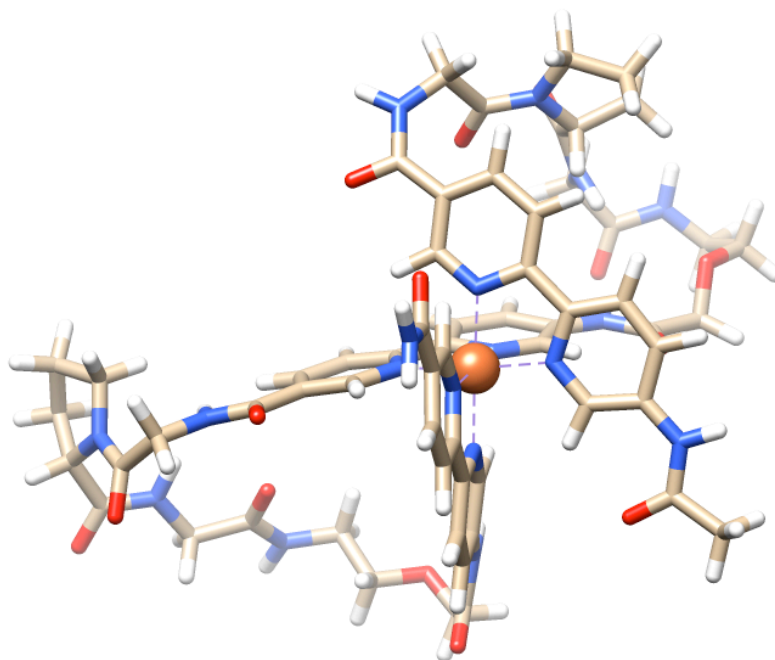


**Figure S37.** Representation of the  $[\text{Fe}(\text{DL-P})]^{2+}$  metalloprotein with the  $\Delta^3$  geometry. In contrast to that observed in the most stable isomer of this system ( $\Delta^4$ , shown in the figure 3 of the manuscript), this isomer has both Pro residues in trans configuration and the loops more exposed to the solvent.

## CD/DFT studies

We calculated the UV-CD spectra of  $[\text{Fe}(\text{LD-P})]^{2+}$  metalloprotein with TD-DFT (CAM-B3LYP//SVP). To this end, on each of the 10 structures described in the above section and depicted in Figure S30, we isolated the bipyridyl chromophores (in red in Figure S37), pruning them at the amide groups and substituting the next C-atom attached either to N or to carbonyl with a hydrogen.

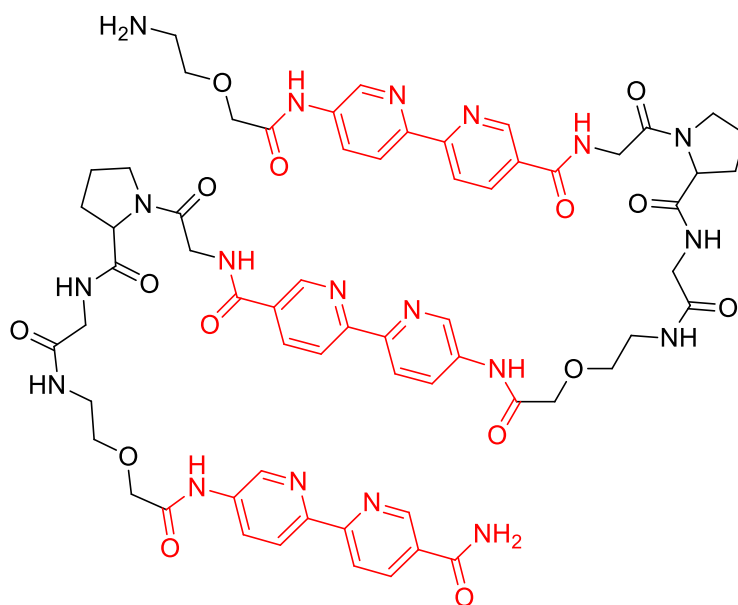


**Figure S38.** Red bonds depict the chromophores of  $[\text{Fe}(\text{LD-P})]^{2+}$  metalloprotein retained for CD calculations. In all cases the first carbon atom up- or downstream the chromophore is substituted with a hydrogen.

All the H atoms were re-optimized with DFT (CAM-B3LYP//SVP), clamping all the remaining atoms to their original positions.

The CD spectra were calculated by TD-DFT at the same level. A Gaussian band shape with 0.25 eV exponential half-width and a red shift of 30 nm were applied to each spectrum. The results are depicted for  $\Delta$ -isomers in Figure S38 and for  $\Lambda$ -isomers in Figure S39. We then averaged the 10 spectra with Boltzmann weights estimated from the energy values of the previous section and depicted in Figure 3 (main text), with the final result shown in Figure S40.

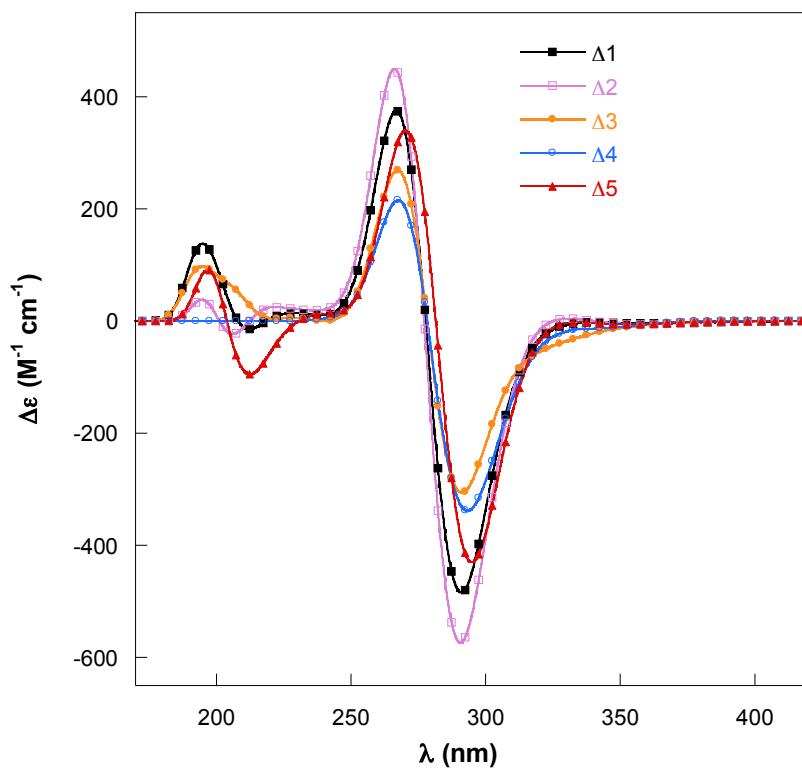


**Figure S39.** Calculated CD spectra for each individual isomer of  $[\text{Fe}(\text{LD-P})]^{2+}$  metallopeptide with  $\Delta$ -configuration

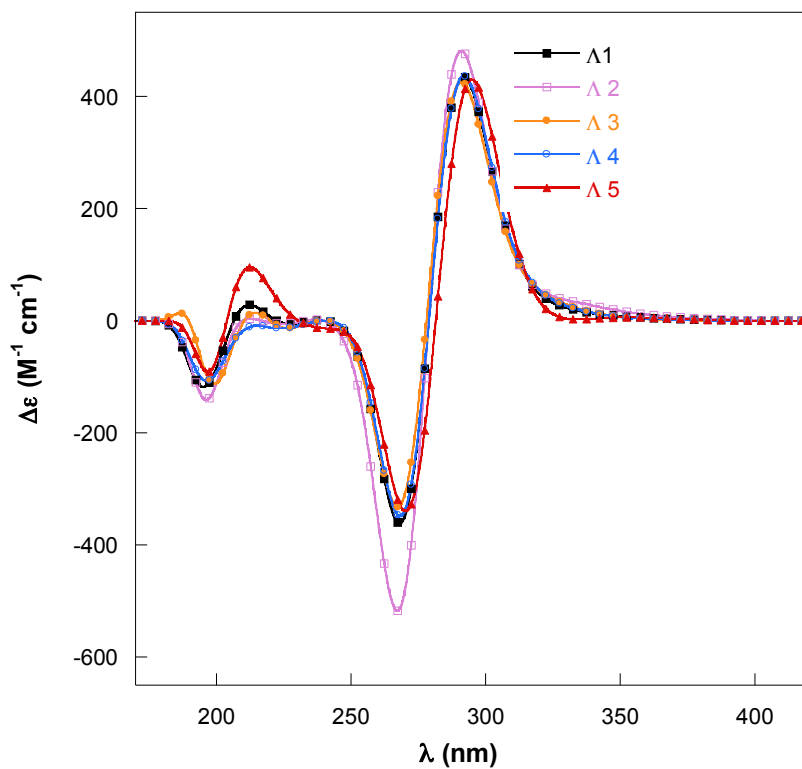


**Figure S40.** Calculated CD spectra for each individual isomer of  $[\text{Fe}(\text{LD-P})]^{2+}$  metallopeptide with  $\Lambda$ -configuration

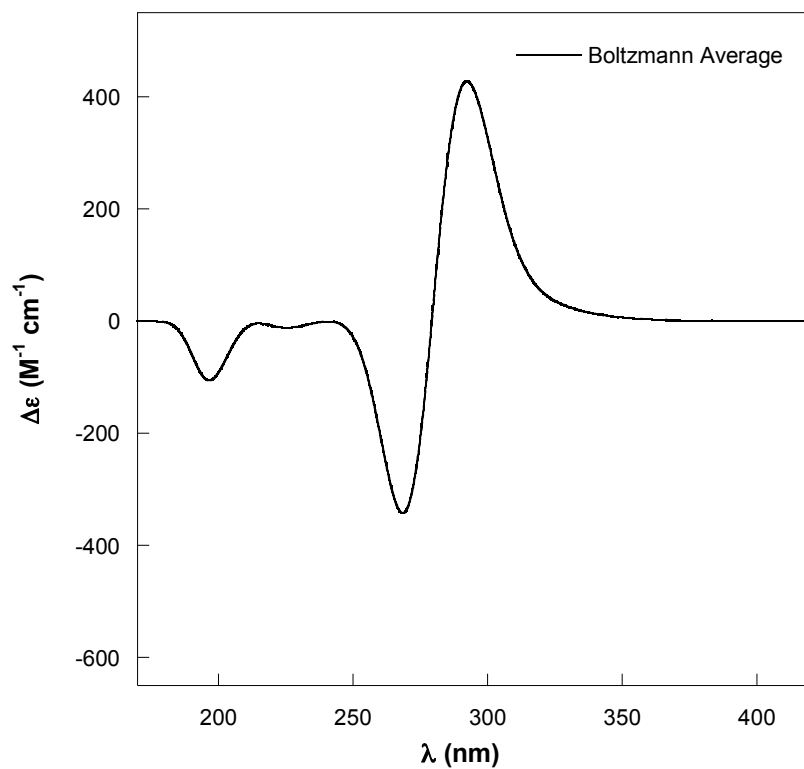


**Figure S41.** Boltzmann-averaged CD spectrum over the 10 conformers described above for [Fe(LD-P)]<sup>2</sup>